Thermal behaviors of clay minerals as key components and additives for fired brick properties: A review

Article *in* Journal of Building Engineering · December 2022

DOI: 10.1016/j.jobe.2022.105802

6 authors, including:

Sen Wang
Queensland University of Technology
20 PUBLICATIONS **588** CITATIONS

SEE PROFILE

Ian Mackinnon
Queensland University of Technology
227 PUBLICATIONS **3,440** CITATIONS

SEE PROFILE

Yunfei Xi
Queensland University of Technology
268 PUBLICATIONS **11,769** CITATIONS

SEE PROFILE

Thermal behaviors of clay minerals as key components and additives for fired brick properties: A review

Sen Wang, Lloyd Gainey, Ian D.R. Mackinnon, Charlotte Allen, Yuantong Gu, Yunfei Xi

PII: S2352-7102(22)01808-3

DOI: https://doi.org/10.1016/j.jobe.2022.105802

Reference: JOBE 105802

To appear in: *Journal of Building Engineering*

Received Date: 18 September 2022

Revised Date: 22 December 2022

Accepted Date: 27 December 2022

Please cite this article as: S. Wang, L. Gainey, I.D.R. Mackinnon, C. Allen, Y. Gu, Y. Xi, Thermal behaviors of clay minerals as key components and additives for fired brick properties: A review, *Journal of Building Engineering* (2023), doi: https://doi.org/10.1016/j.jobe.2022.105802.

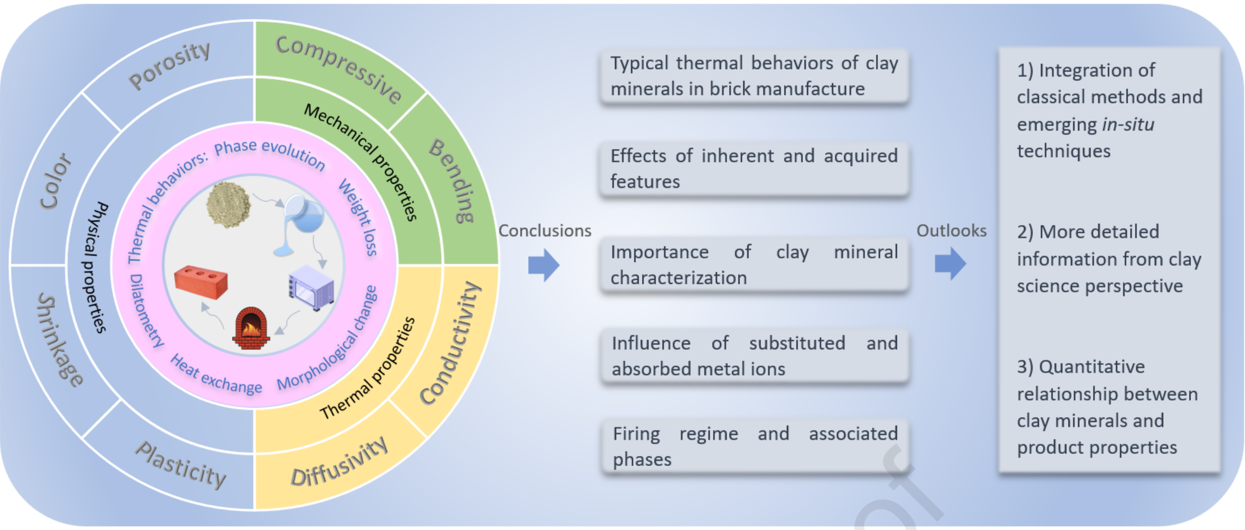

Typical thermal behaviors of clay minerals in brick manufacture

Effects of inherent and acquired features

Importance of clay mineral characterization

Influence of substituted and absorbed metal ions

Firing regime and associated phases

1) Integration of classical methods and emerging *in-situ* techniques

2) More detailed information from clay science perspective

3) Quantitative relationship between clay minerals and product properties

Thermal behaviors of clay minerals as key components and additives for fired brick properties: A review

Sen Wang [b, e], Lloyd Gainey [c], Ian D. R. Mackinnon [b, d], Charlotte Allen [a, d], Yuantong Gu [f] and Yunfei Xi [a, b, e*]

[a] Central Analytical Research Facility (CARF), Queensland University of Technology (QUT), Brisbane, Queensland 4001, Australia

[b] Centre for Clean Energy Technologies and Practices & Centre for Materials Science, Queensland University of Technology (QUT), Brisbane, Queensland 4001, Australia

[c] Brickworks Ltd. & Austral Bricks, Rochedale, Queensland 4123, Australia

[d] School of Earth and Atmospheric Sciences, Queensland University of Technology (QUT), Brisbane, Queensland 4001, Australia

[e] School of Chemistry and Physics, Queensland University of Technology (QUT), Brisbane, Queensland 4001, Australia

[f] School of Mechanical, Medical and Process Engineering, Queensland University of Technology (QUT), Brisbane, Queensland 4001, Australia

*Corresponding author

E-mail address: y.xi@qut.edu.au (Y. Xi)

Post address: Room 605C, Level 6, P block, Gardens Point Campus, Queensland University of Technology, Brisbane, QLD 4001, Australia

Abstract

Clay minerals are critical components for fired bricks because they provide plasticity, porosity and adequate strength for desired products. Investigations on clay minerals have been extensively published but those relevant to bricks have not been systematically reviewed in recent decades. Nowadays, the global brick industry faces critical challenges from energy costs, regulatory policies, and competing materials. A full understanding of raw materials for brick making is crucial for precise quality control and mitigation of waste streams. The innovative use of non-clay additives has substantially enhanced performance or processing conditions. However, moderating existing clay minerals may provide a more practical solution for many producers. This review summarizes recent progress in clay mineral-related brick production. Firstly, eight typical clay minerals are grouped according to their roles in the brick-making raw material. Research progress on the thermal behaviors of these clay minerals is summarized, including thermal mass loss, thermal phase transition, thermal expansion/shrinkage, etc. Then, relationships between clay minerals and critical physical, mechanical, and thermal conductivity/diffusivity characteristics of clayey raw materials and obtained brick products are comprehensively reviewed. Relevant studies on mineralogy and porcelain/earthenware products have also been perused to present an interdisciplinary conclusion. Finally, the current challenges in clay mineral-related brick production and potential suggestions are proposed. This review aims to provide a reference for designing clay mixtures and clay-based additives that deliver enhanced properties of bricks produced at an industrial scale.

Keywords

Clay mineral; Fired brick; Thermal behavior; Physical and mechanical properties; Thermal conductivity/diffusivity

Abbreviations

DSC	Differential scanning calorimetry
DTA	Differential thermal analysis
DTD	Derivative thermodilatometry
DTG	Derivative thermogravimetry
FT-IR	Fourier-transform infrared spectroscopy
NMR	Nuclear magnetic resonance
R&D	Research and development
SEM	Scanning Electron Microscopy
TD	Thermodilatometry
TEM	Transmission electron microscopy
TGA	Thermogravimetric analysis
XRD	X-ray diffraction
XRF	X-ray fluorescence
EDS	Energy dispersive X-ray spectroscopy

1. Introduction

Clay minerals are a diverse group of hydrous aluminosilicates that usually display layered or fibrous structures encompassing polymeric sheets of silica tetrahedra linked with octahedral sheets [1]. Clay minerals have received considerable attention in the past decades because of their appealing properties, such as natural abundance, high reactivity, and low cost [2]. The versatility and significance of clay minerals are reflected by their broad applications in environmental science, industrial and geological settings, and even roles in the origins of life [3]. Among all these, the application of clay minerals for fired brick manufacturing is the most common and has consumed the bulk of clay mineral reserves throughout human history. According to Mohajerani, et al. [4], 3.13 billion cubic meters of clay soils are consumed for the annual production of 1,500 billion bricks globally and brick production is still increasing, particularly in developing countries.

In recent years, although clayey materials have been partially replaced by solid wastes in order to reduce costs and to preserve cultivated land and the environment, the amount of added solid waste is commonly less than 30 wt.% because higher addition would likely lead to substandard products [5]. Clay minerals thus remain primary and crucial components of the starting materials to produce bricks.

Clay minerals can endow plasticity to the clayey earth which can be kneaded into a brick shape with water [6, 7]. The vitrification of clay minerals under high temperatures generates glass phases to densify the brick body. Nearly all the performance of bricks, including physical, mechanical, and thermal diffusivity/conductivity properties, can be affected by clay minerals [8-10]. On the other hand, an improper selection/proportions of clay minerals may result in various defects in bricks, such as cracking and deformation.

Since most clay minerals are weathering products from natural processes, they possess variable structures and chemistry, which adds complexity to their roles in brick fabrication. Brick manufacturers have gained a great deal of priceless first-hand experience from production for more than 6500 years but sophistication has not always ensued due to a hesitation to employ adequate high-end testing equipment on the factory floor [11]. Furthermore, many researchers collect clayey earth from specific locations of limited compositional variability to evaluate brick making [12, 13]. The resultant product may not be a factory floor model but a relatively oversimplified laboratory result.

Although the types and concentrations of clay minerals might be qualitatively or quantitatively analyzed, with some thermal behaviors tracked, the connection between clay minerals and technological properties of obtained bricks has seldom been discussed, especially with respect to the relative contribution of different types and mixtures of clay minerals. Consequently, the case-by-case studies presented may aid better utilisation of local clayey earth, while recognizing that specific observations here may have limited influence on real production practices. A common difficulty of directly translating these case studies to other localities rests with inconsistencies in starting materials; clay minerals in different regions/pits have varying compositions and crystallinity, and their nature is often not disclosed (or measured) in many studies.

In some recent reports, researchers have attempted to analyze the explicit functions of different clay minerals by artificially adjusting their concentrations in the clayey raw materials [14-19]. Although most of these studies are preliminary, they are addressed in this review due to their wide applicability. In addition, the advance in modern characterization techniques has inspired numerous studies on the thermal behavior of clay minerals [20-22]. From a material science perspective, these studies were not conducted to develop bricks/tiles but for fundamental mineralogical investigation or porcelain/earthenware fabrication. Compared to brick making, the raw materials to produce porcelain usually exhibit finer particle size and greater amounts of clay minerals. A higher calcination temperature (e.g., < 1600 °C instead of < 1200 °C used for brick making) is also commonly reported. However, the thermal behavior of clay minerals, especially the change of physical and chemical properties during firing, is similar to firing bricks and can provide valuable reference points. Furthermore, mineralogical investigation, such as using high-temperature phase diagrams, can profitably be used to predict possible phases/phase changes in manufactured bricks.

Thus, in this review, an interdisciplinary perspective has been adopted, covering building materials, ceramic materials, and mineralogy research (**Fig. 1**). Previous reviews have concentrated on various industrial and/or agricultural wastes as additives during brick production [23-25]. In this work, the functions of clay minerals as primary components or additives are specifically emphasized and summarized, including 1) thermal behaviors of different clay minerals and 2) influences of thermal behaviors on physical, mechanical and thermal conductivity/diffusivity properties of brick products. Based on present knowledge, prospects for further work to address the problems and challenges in this field are also provided.

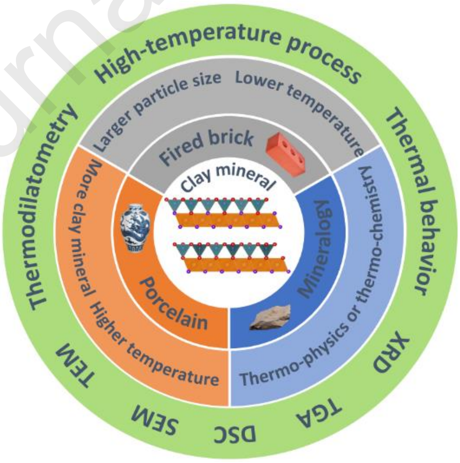

Fig. 1. Comparisons of raw materials, processing conditions, and characterization techniques when clay minerals are applied for multidisciplinary fields, including fired brick, porcelain and mineralogy research.

2. Definition and classification of clays and clay minerals

Historically, “clay” and “clay mineral” are frequently interchanged by those unfamiliar with this distinctive terminology. However, these two terms should be distinguished for a better understanding of the relationship between clayey materials and brick manufacture.

According to Bergaya and Lagaly [2], clay minerals are “phyllosilicate minerals and minerals which impart plasticity to clay and which harden upon drying and firing”. Although clay minerals behave similarly based on this definition, they are classified into different groups based on their structural and chemical characteristics, e.g., unit type, interlayer matter and charges. The Clay Mineral Society published the latest classification of planar hydrous phyllosilicates (the most common type of clay mineral) in 1991 [26]. Eight different groups were defined, including the serpentine-kaolin group, talc-pyrophyllite group, smectite group, vermiculite group, true (flexible) mica group, brittle mica group, chlorite group, and a regularly interstratified clay mineral group. The structure of typical minerals in these groups is shown in **Fig. 2**, and their thermal behaviors (except for the interstratified clay mineral group) are discussed in a parallel fashion in Section 3. In addition, a non-planar hydrous phyllosilicate - the sepiolite-palygorskite group - is included in Section 3 due to the abundant worldwide reserves (**Fig. 2g** and **2h**).

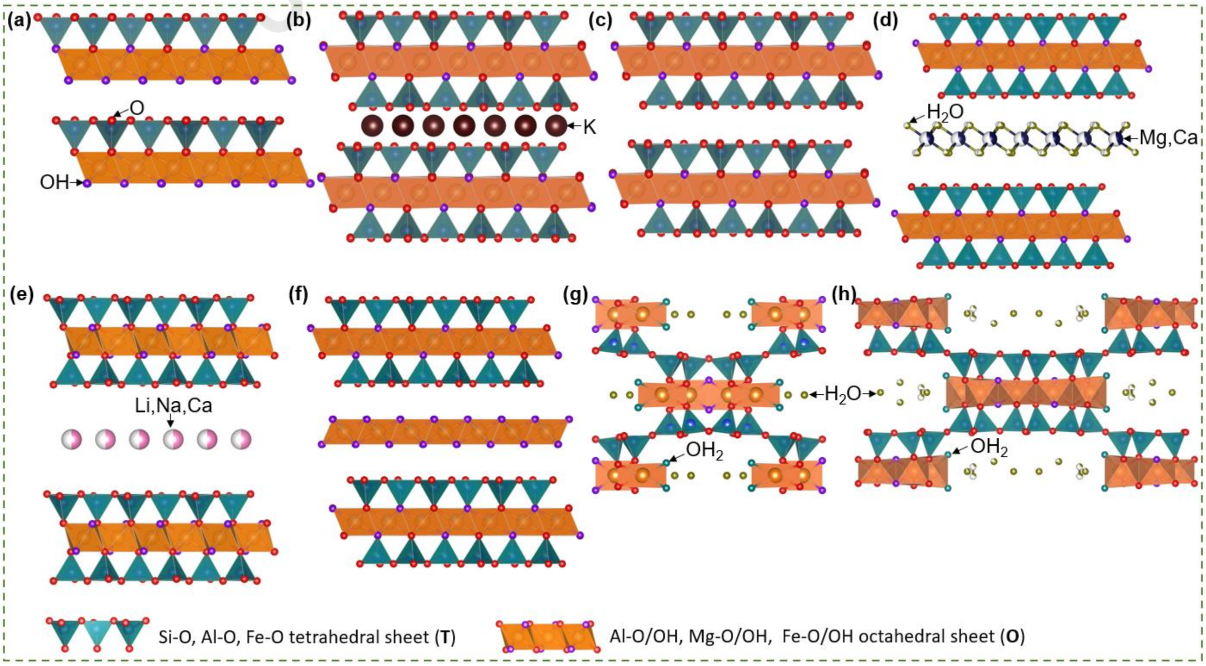

Fig. 2. Structural schematics for different clay minerals [2]. Reproduced with permission. Copyright 2013, Elsevier. (**a**) kaolinite, halloysite and serpentine: T-O 1:1 layers; (**b**) illite: T-O-T 2:1 layers; (**c**) talc and pyrophyllite: T-O-T 2:1 layers; (**d**) vermiculite: T-O-T 2:1 layers; (**e**) montmorillonite: T-O-T 2:1 layers; (**f**) chlorite: T-O-T-T 2:1:1 layers; (**g**) palygorskite: T-O-T 2:1 layers; (**h**) sepiolite: T-O-T 2:1 layers.

Since most clay minerals are formed naturally, they are associated with other phases, such as carbonates, feldspars, quartz, hydroxides of iron and aluminum, and non-crystalline phases. These associations give rise to another term capturing the multi-phase mixtures found in nature - “clay”: a naturally occurring material composed primarily of fine-grained minerals, which is generally plastic at appropriate water contents and will harden when dried or fired [2].

According to the above definition, clay minerals are predominant components of clay, and clay is a conventional and preferred raw material for brick/tile fabrication. Fired clay bricks are produced from various mixes of clays/clayey raw materials, pressed/extruded, dried and, subsequently, fired [9].

The crucial role of clay minerals in brick manufacturing requires a clear understanding of precise relationships between a specific mineral’s thermal behavior and final brick properties for optimized clay mix design. In this work, these key relationships are detailed in Sections 3 to 6 (also shown in the Graphical Abstract). Given that clay minerals are a non-renewable resource, efficient utilization of local clay/clay minerals may result in significant economic benefits for brick manufacturers.

3. Thermal behaviors of clay minerals

In this section, the progress in characterization of thermal behaviors of typical clay minerals in the temperature range(s) relevant to brick manufacture have been summarized for the period 1935-2022. These thermal behaviors, including phase transitions, mass loss, heat exchange, dimensional and morphological changes, can endow beneficial or detrimental key features on brick bodies. However, only clay minerals that have been reported in fired brick/ceramic manufacture (either as primary components in Section 3.1 or impurities/additives in Section 3.2) are included, considering that not all clay minerals belong to the paragenesis of clay deposits that are commonly used to make bricks.

In particular, due to the importance of thermal shrinkage/expansion of the brick body, dilatometric curves for clay minerals are reproduced from the literature in a format that allows ready comparison (**Fig. 3**). By understanding thermal behaviors, clay materials with variable characteristics can be judiciously combined for optimized manufacture of functional brick products.

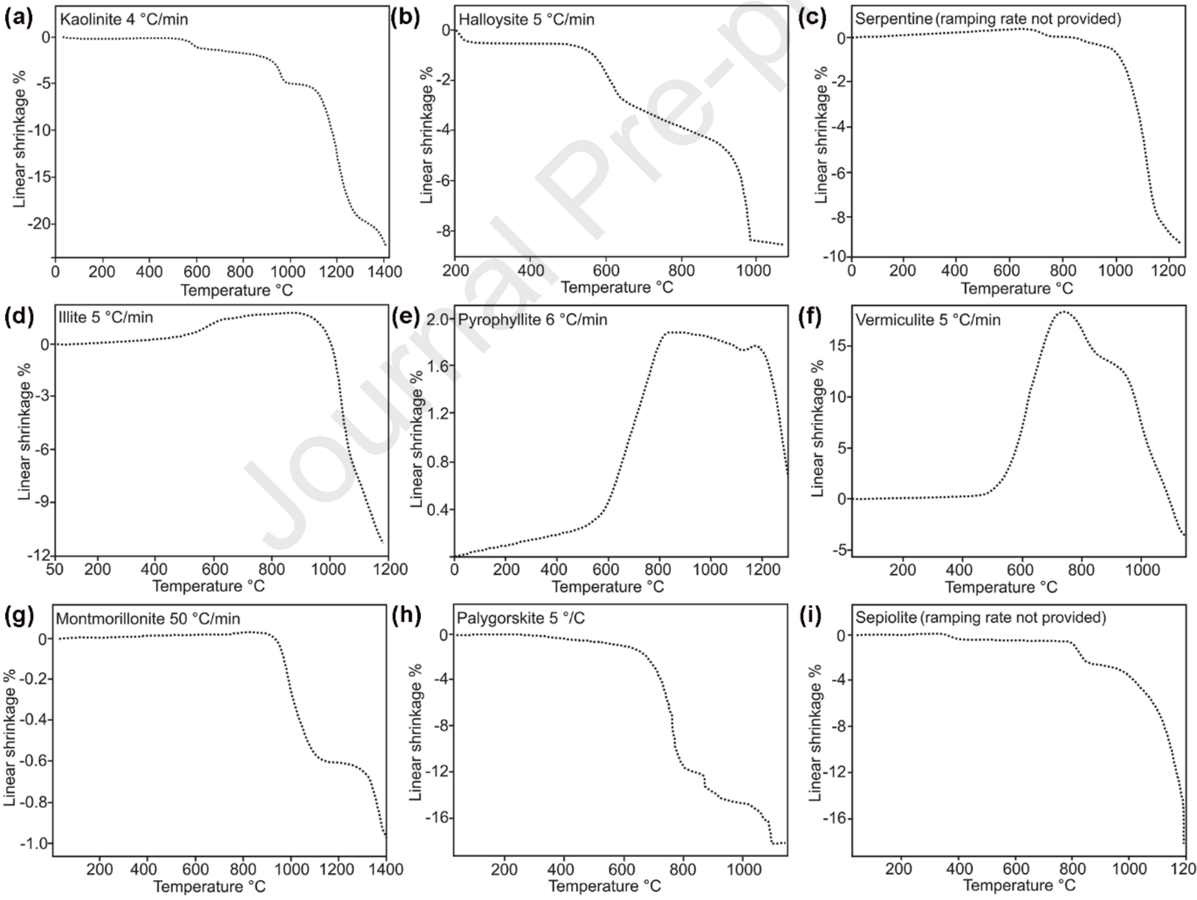

Fig. 3. Thermodilatometric (TD) curves of clay minerals. (**a**) kaolinite [27]; (**b**) halloysite [28]; (**c**) serpentine [29]; (**d**) illite [30]; (**e**) pyrophyllite [31]; (**f**) vermiculite [14]; (**g**) montmorillonite [22]; (**h**) palygorskite [9]; (**i**) sepiolite [32]. (**a**)-(**i**) are reproduced with permission.

3.1. Primary clay minerals in brick making

3.1.1. Kaolinite and halloysite

Kaolinite and halloysite are both serpentine-kaolin group clay minerals with a similar crystal structure (**Fig. 2a**). Although kaolinite usually exhibits a hexagonal morphology while halloysite is typically tubular, similar mineralogical and chemical characteristics of kaolinite and halloysite result in comparable thermal behaviors. In this section, the thermal evolution of kaolinite will be primarily discussed given that kaolinite is more abundant in nature than halloysite.

Kaolinite with the ideal formula of $Al_2Si_2O_5(OH)_4$ is primarily formed by weathering, hydrothermal alteration, or sedimentation [33]. Kaolinite is a common 1:1 type layered phyllosilicate with a crystal structure consisting of SiO_4 tetrahedral sheets and $AlO_2(OH)_4$ octahedral sheets in a periodic array along the c-axis. As an essential ingredient in manufacturing whiteware, kaolinite has been widely reported as the basis for china and porcelain, and commonly occurs in raw materials for brick production. Previous literature reports that kaolinite as a mono-phase undergoes four structural changes during heating as follows [34]:

1) Low-temperature reaction (< 400 ℃);
2) Intermediate-temperature reaction (400-650 ℃);
3) High-temperature reaction (> 700 ℃);
4) Oxidation reaction.

A slight mass loss at temperatures below 400 ℃ is caused by the evaporation of water physically absorbed on the external surfaces of kaolinite. In the intermediate-temperature region, kaolinite dehydroxylates to form metakaolinite. The $AlO_2(OH)_4$ octahedron in kaolinite migrates into the inter-layer spacing during dehydroxylation, resulting in a localized buckling of the 1:1 Al-Si layers; thus, the (001) XRD reflection disappears. The structure of metakaolinite does not entirely collapse along the *c* axis, and the pseudohexagonal morphology remains as confirmed by TEM observation [35]. MacKenzie, et al. [36] reported that around 10% of hydroxyl groups, which are likely the inner hydroxyls, remain within metakaolinite to support a partial short-range order. In addition, the DTG or DTA peak, which reflects the dehydroxylation temperature of kaolinite, displays some variability caused by a few factors such as crystallinity [37], heating rate [38], pressure [39] and milling treatment [40].

As heating proceeds, a cubic γ-Al_2O_3 spinel phase crystallizes within metakaolinite accompanied by the formation of amorphous SiO_2. The composition of the spinel phase is debated (whether Al-spinel or Al-Si spinel) while two spinel types were proposed by Ghorbel, et al. [41] according to the following reactions:

$$Al_2O_3 \cdot 2SiO_2 \xrightarrow{950-1000\,℃} SiAl_2O_5\ (Al - Si\ spinel)\ +\ SiO_2\ (amorphous) \qquad (1)$$

$$Al_2O_3 \cdot 2SiO_2 \xrightarrow{950-1000\,℃} Al_2O_3\ (\gamma - alumina\ spinel)\ +\ 2SiO_2\ (amorphous) \qquad (2)$$

Lee, et al. [42] reported that the spinel phase might have a topotactic relationship with metakaolinite. In addition, a trace of weakly crystalline mullite is identified as occurring in parallel with spinel. Thus, the exothermic peak at ~980 ℃ may be attributed to the nucleation of mullite, rather than the formation of spinel-type phases [42].

At about 1100-1200 ℃, spinel is lost and elongated mullite crystals begin to develop:

$$SiAl_2O_5(Al - Si\ spinel) + SiO_2(amorphous) \rightarrow \tfrac{1}{3}3Al_2O_3 \cdot 2SiO_2\ (mullite) + \tfrac{4}{3}SiO_2\ (amorphous)$$

(3)

$$Al_2O_3(\gamma - alumina) + SiO_2(amorphous) \rightarrow \frac{1}{3}3Al_2O_3 \cdot 2SiO_2\ (mullite) + \frac{4}{3}SiO_2(amorphous)$$

(4)

This phenomenon was confirmed with both powder and extruded kaolinite samples as described from relevant TEM observations in the schematic shown in **Fig. 4a**.

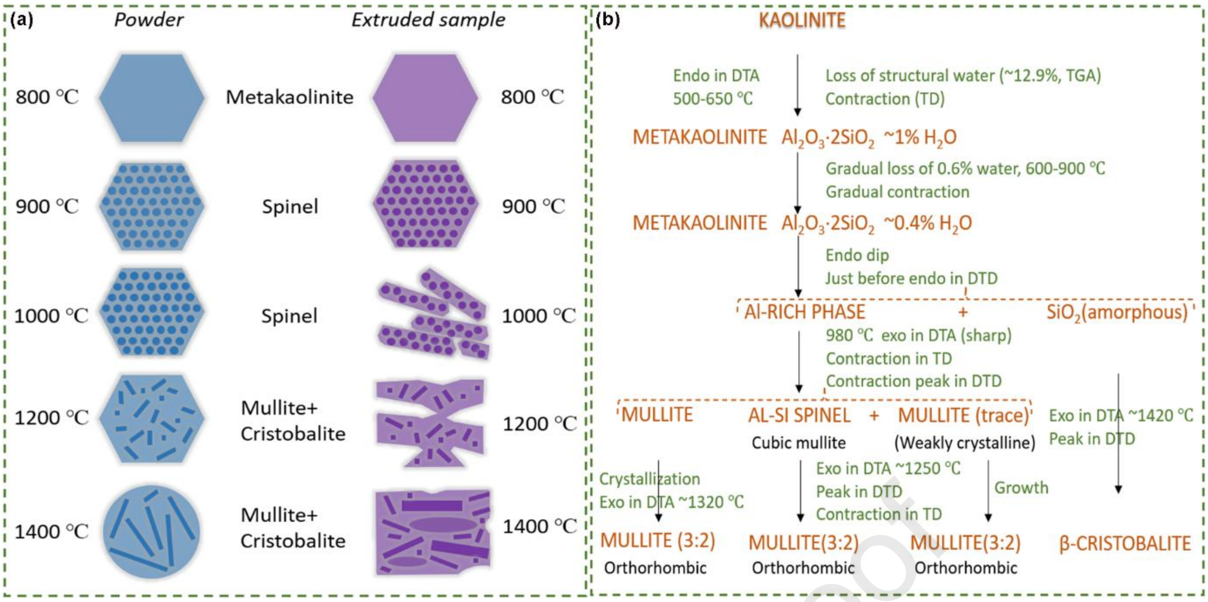

Fig. 4. (**a**) Schematic diagram of the thermal evolution of kaolinite powder and extruded samples observed by TEM; (**b**) Reaction sequences of the decomposition of kaolinite. (**a**) and (**b**) are cited from [43]. Reproduced with permission.

In addition, the size and amount of microcrystalline mullite particles increase with temperature (**Fig. 4a**), and the formed mullite can improve brick strength due to their acicular morphology and interlinked arrangement of crystals. The mullite crystalized from kaolinite tends to be smaller than that from illite and montmorillonite and a possible reason is the lack of alkali and alkaline earth metals (e.g. K, Na and Fe); these elements can promote the formation of fluid silicate liquid and facilitate mullite crystal growth [21]. At temperatures >1200 °C, cristobalite begins to form from amorphous SiO_2 (**Fig. 4a**), until eventually mullite and cristobalite are the only remaining crystalline phases, with alkali and alkaline earth metal elements partially integrated into their structures.

Reaction sequences of decomposition of kaolinite are summarized from low to high temperature in **Fig. 4b**. Importantly, since kaolinite is not the only mineral in common brick-making starting materials, it will react with other phases at high temperatures. Thus, the phase change sequence and the type of phases may change. Typical high-temperature phases derived from kaolinite in the presence of co-phases are summarized in **Table 1**.

Table 1. High-temperature phases derived from kaolinite and other phases.

Raw material	Firing regime	Final product	Reference
Kaolinite and calcite	800 ℃ for 3h	gehlenite	[44]
Kaolinitic clay (75 vol.%) and limestone (25 vol.%)	1000 ℃ for 1h	gehlenite	[45]
Kaolin (46 wt.%), serpentine waste (9 wt.%), and kiln roller waste (45 wt.%)	1450 ℃ for 2h	cordierite and mullite	[46]
Kaolinite: Al_2O_3 powder = 2:1 (molar ratio)	1600 ℃ for 4h	mullite and alumina	[47]
Kaolinite and gibbsite mixed as a stoichiometric mullite composition	1300 ℃ for 2h	α-alumina and mullite	[48]
Kaolinite and boehmite mixed as a stoichiometric mullite composition	1200-1300 ℃ for 2h	mullite	[48]
Kaolinite: Na_2CO_3 = 1:1.2 (molar ratio)	900 ℃ for 2h	nepheline and zeolite	[49]
Kaolin (50 wt.%), talc (20 wt.%) and bauxite (30 wt.%)	1400 ℃ for 2h	cordierite, mullite, cristobalite and pseudorutile	[50]
Kaolinite, talc and alumina	1300 ℃ for 2h	cordierite, corundum, cristobalite, quartz and mullite	[51]
Kaolin (75 wt.%) and waste serpentine (25 wt.%)	1300 ℃ for 2h	cordierite and enstatite	[52]

In addition, TD analysis shows that kaolinite experiences a series of contractions in different transformation stages, except for one expansion step. A typical dimensional change of kaolinite between 25-1400 ℃ is shown in **Fig. 3a** and follows the sequence [22, 27, 53]:

1) A minor contraction (~0.05%) at < 150 ℃ due to the loss of surface adsorbed water;
2) A linear thermal expansion of 0.2%-0.3% up to 470-550˚C (depending on the heating rate) due to lattice expansion;
3) The first rapid shrinkage (1.0%-1.8%) between ~500 ℃ and ~650 ℃ due to dehydroxylation;
4) A less harsh shrinkage (1.5%-2.3%) at ~650-900 ℃;
5) The second rapid shrinkage (1.0%-3.7%) between ~900 ℃ and ~1000 ℃ due to collapse of the metakaolinite lattice and the formation of spinel and mullite;

6) A slow shrinkage or sometimes stable length at ~1000-1100 ℃;

7) The third sharp shrinkage (~17.5%) between 1100 ℃ and 1400℃ due to solid-sate sintering accompanied by crystallization of mullite and cristobalite.

3.1.2. Illite

The structure of illite is composed of two opposing tetrahedral sheets with an octahedral sheet in between to form a 2:1 layer phyllosilicate (**Fig. 2b**). In illite, the substitution of Al^{3+} for Si^{4+} occurs in tetrahedral sheets with the charge balanced by interlayer K^+ (**Fig. 2b**). Rieder, et al. [54] proposed a formula for illite: $(K\ Na)_{x+y}(Mg\ Fe^{2+})_x(Al\ Fe^{3+})_{2-x}\ [Si_{4-y}Al\ Fe^{3+}{}_y]O_{10}(OH)_2$, where $0.6 \leq x+y \leq 0.85$.

The thermal behavior of illite has been widely studied [20, 21, 30, 55]. *In-situ* high-temperature XRD shows that illite dehydroxylates at 525-575 ℃ in air followed by a structural collapse after 1125 ℃ with the formation of mullite and amorphous phases (**Fig. 5a**).

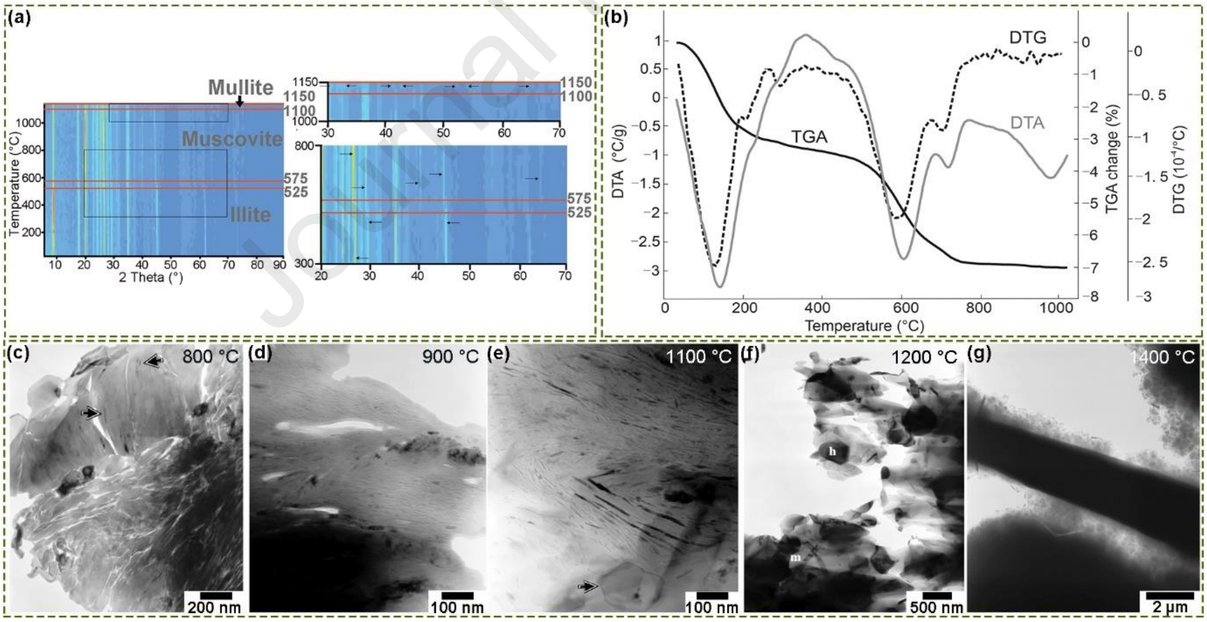

Fig. 5. (**a**) Isolines of *in-situ* XRD patterns for illite showing three stable thermal ranges (illite, muscovite and mullite) in static air [20]; (**b**) DTA, TGA and DTG curves of illite [56]; (**c**) Bright-field (BF) TEM image of illite clay fired 3h at 800 °C showing lath-like structures and spinel crystals (arrowed); (**d**) 3h at 900 °C showing topotactically crystallized spinel; (**e**) 3h at

1100 °C showing apparently elongated spinel crystals and hematite (arrowed); (**f**) 3h at 1200 °C, ≈100 nm pseudohexagonal hematite crystals can be seen; (**g**) 3h at 1400 °C showing >10 μm mullite needles surrounded by amorphous phase containing. (**c**)-(**g**) come from [21]. (**a**)-(**g**) are reproduced with permission.

Different dehydroxylation temperatures have been identified depending on test conditions, instrument parameters, particle size and structures of species, which have been summarized by Wang, et al. [20]. Antal, et al. [56] also observed two distinct peaks at around 600 ℃ and 750 ℃ on the DTG and DTA curves representing the dehydroxylation of *trans*-vacant and *cis*-vacant sheets (**Fig. 5b**).

After dehydroxylation, the (002) reflection of illite remains in the XRD pattern. Dehydroxylated illite presents a lath-like morphology with the appearance of elongated spinel in Al- or Mg-rich micro-domains (an octahedral relict after the destruction of the illite structure) (**Fig. 5c-5e**). Liquid phases also occur in the Si-rich micro-domain (the tetrahedral relict and the K^+ from illite interlayer) [21, 57], but spinel has not been identified when the few illite-only samples were fired [20, 58].

With increased temperature, the liquid phase grows dramatically due to the continuous melting of illite and then mullite starts to form after enough alkali atoms have migrated from illite to its surrounding low alkali matrix. Mullite crystals precipitated in illite usually contain more Fe and are larger than that from kaolinite (**Fig. 5g**). The reported formation temperatures for mullite differs, e.g., 1100 ℃ [58], 1125 ℃ [20] or 1200 ℃ [21].

Due to common substitution of Al by Fe in the original illite structure, Fe-dominated minerals such as hematite and ilmenite may develop under high temperatures (**Fig. 5e** and **5f**). This may change the color of bricks as discussed in Section 4.1.4. Cristobalite, on the other hand, does not normally appear when illite is fired and instead Ca-containing phases and mullite may be formed through reactions between illite and its associated minerals [59]:

$$KAl_2(Si_3Al)O_{10}(OH)_2(illite) + 6CaCO_3(calcite) \xrightarrow{800\ ℃} 3Ca_2Al_2SiO_7(\text{gehlenite}) + 6CO_2 + 2H_2O + K_2O + 3SiO_2 \quad (5)$$

$$KAl_2(Si_3Al)O_{10}(OH)_2(illite) + 2CaCO_3(calcite) + 4SiO_2(quartz) \xrightarrow{900\ ℃} 2KAlSi_3O_8(K-feldspar) + 2Ca_2Al_2SiO_8(anorthite) + 2CO_2 + H_2O \quad (6)$$

$$3KAl_2(Si_3Al)O_{10}(OH)_2(illite) + 2SiO_2 \xrightarrow{1000-1100\ ℃} 3KAlSi_3O_8(sanidine) + Al_6Si_2O_{13}(mullite) + 3H_2O \quad (7)$$

Due to the common presence of Ca in clayey materials which participates in the formation of high-temperature phases during firing, the phase diagram of a CaO-Al_2O_3-SiO_2 system at 1200 ℃ is shown in **Fig. 6a,** with typical Ca-containing high-temperature phases included. The gehlenite formed in equation 5 may incorporate Fe in its structure and causes dingy colors in fired brick products.

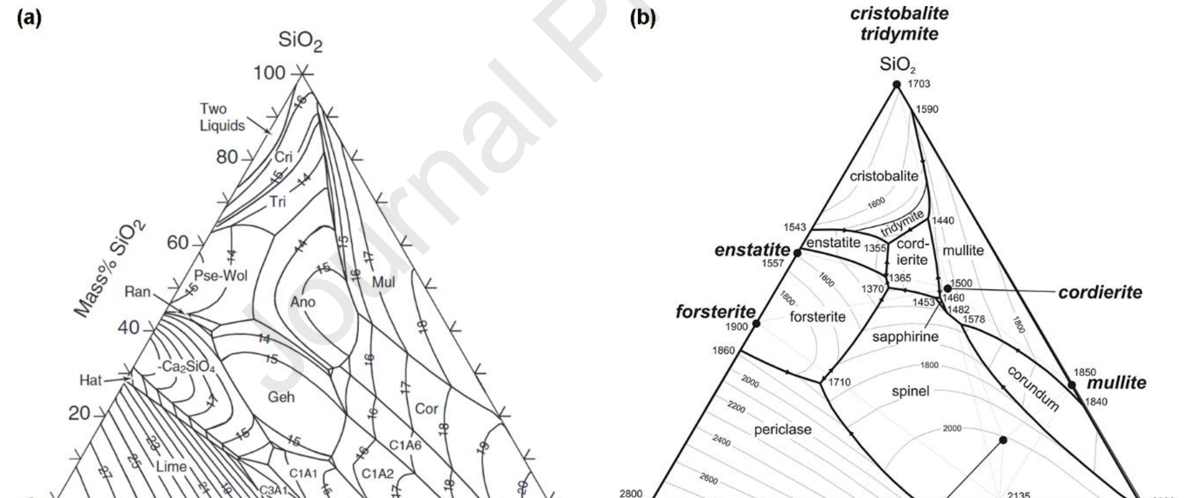

Fig. 6. Phase diagrams of (**a**) CaO-Al_2O_3-SiO_2 system. Ano, anorthite; C_1A_1, CaO·Al_2O_3; C_1A_2, CaO·2Al_2O_3; C_1A_6, CaO·6Al_2O_3; C_3A_1, 3CaO·Al_2O_3; Cor, corundum; Cri, cristobalite; Geh, gehlenite; Hat, Hatrurite; Mul, mullite; Pse-Wol, pseudo-wollastonite; Ran, rankinite; Tri, tridymite [60]; (**b**) MgO-Al_2O_3-SiO_2 system [61]. (**a**) and (**b**) are reproduced with permission.

As for the TD curve for illite (**Fig. 3d**), six steps are summarized for dimensional changes during constant heat input [22, 62-64]:

1) 25-200 ℃, a small contraction due to the release of physically bound water;
2) 200-500 ℃, a slow and linear expansion because of lattice expansion;
3) 500-650 ℃, a sharp expansion resulting from dehydroxylation of illite and sometimes α→β transition of quartz impurity;
4) 650-850 ℃, a nearly unchanged dimension;
5) 850-1100 ℃, melting of illite with the formation of spinel;
6) 1100-1200 ℃, melting of illite with mullite crystallization.

3.2. Clay minerals as impurities and additives

Apart from kaolinite, halloysite and illite, other clay minerals can occur in starting materials - either inadvertently due to provenance or deliberately - as part of the brickmaking process. These other clay minerals may be viewed either as impurities or as intended additives, respectively. The total content of these clay minerals in the starting material mix is normally less than 20 wt.% but specific thermal behaviors of some such phases may affect brick performance, so this section summarizes the thermal behaviors of key clay minerals.

3.2.1. Talc

Talc is a natural flux material with a 2:1 trioctahedral layers comprised of two tetrahedral SiO_4 sheets separated by an octahedral $MgO_4(OH)_2$ sheet (**Fig. 2c**). Upon heating, dehydration of talc occurs between 25-700 ℃. Then, talc dehydroxylates at ~800-1000 ℃ as shown by reaction 8 below:

$$2Mg_3Si_4O_{10}(OH)_2 \rightarrow 6MgSiO_3(enstatite) + 2SiO_2(amorphous) + 2H_2O \quad (8)$$

At 1200 ℃, opal-CT (disordered microcrystalline cristobalite in a matrix of amorphous silica) and clinoenstatite crystallize from the amorphous SiO_2 and enstatite formed at lower temperature as shown in reaction 9 [65]:

$$2MgSiO_3(enstatite) + SiO_2(amorphous) + nH_2O\ (g) \rightarrow 2MgSiO_3(clinoenstatite) + SiO_2 \cdot nH_2O(opal - CT) \quad (9)$$

According to Benhammou, et al. [66], talc undergoes a constant thermal expansion up to 800 ℃, while shrinkage manifests above 800 ℃ due to dehydroxylation and decomposition.

3.2.2. Pyrophyllite

Pyrophyllite is a layered dioctahedral 2:1 clay mineral with a unit cell comprising an Al-O(OH) octahedral sheet sandwiched between two SiO_4 tetrahedral sheets (**Fig. 2c**). The thermal behavior of pyrophyllite is straightforward with four steps defined as follows [31, 67]:

1) dehydration of pyrophyllite below ~500 ℃;

2) dehydroxylation of pyrophyllite between ~500 ℃ and ~900 ℃;

3) decomposition of dehydroxylated pyrophyllite at 1000-1100 ℃. The intensities of all pyrophyllite reflections decrease markedly at this point. Meanwhile, poorly ordered mullite may also form at 1100-1150 ℃ according to the following reaction [67]:

$$Al_2O_3 \cdot 4SiO_2(dehydroxylated\ pyrophyllite) \rightarrow 3Al_2O_3 \cdot 2SiO_2(mullite) + SiO_2(amorphous) \quad (10)$$

4) crystallization of mullite and cristobalite at ~1215 ℃ and ~1325 ℃, respectively.

The platy morphology of pyrophyllite remains at 1300 ℃ but disappears after 1430 ℃ [68]. On the TD curve (**Fig. 3e**), similar trends have been reported as summarized below [31, 69]:

1) a linear expansion of ~0.3% between 25 ℃ and ~500 ℃ due to lattice expansion;
2) a sharp expansion of ~1.5% between ~500 ℃ and ~800 ℃ caused by dehydroxylation;
3) a plateau stage between 800 ℃ and 1100 ℃;
4) a slight expansion between 1100-1200 ℃;
5) a shrinkage of ~1.0% at 1200-1300 ℃ caused by decomposition and crystallization of mullite and cristobalite.

3.2.3. Vermiculite

Vermiculite is a 2:1 type layered magnesia aluminosilicate clay mineral consisting of two Al for Si substituted tetrahedral silicate sheets separated by an Al-Fe for Mg substituted octahedral sheet (**Fig. 2d**). A typical formula for idealized vermiculite is $(Mg^{2+}, Fe^{2+}, Fe^{3+})_3[(SiAl)_4O_{10}]OH_2\cdot 4H_2O$ [70]. Vermiculite expands rapidly when heated at around 650-950 °C. Expanded vermiculite can act as a pore-forming agent which produces lightweight thermal insulation bricks.

For a typical Mg^{2+}-vermiculite, an initial (002) basal reflection presents at 14.4-14.8 Å on the XRD pattern depending upon the degree of hydration. This reflection changes to ~10 Å at 400 ℃, suggesting a dehydrated state in the interlayer space. The intensity of the 10 Å reflection decreased above 800 °C and disappeared at 1000 °C, probably because of dehydroxylation [71]. Enstatite also crystallizes after dehydroxylation as shown in reaction 11:

$$2Mg_3(Si_3Al)O_{10}(OH)_2(vermiculite) \rightarrow 6MgSiO_3(enstatite) + Al_2O_3 + H_2O \tag{11}$$

The SiO_2-Al_2O_3-MgO phase diagram shows that vermiculite can lead to high-temperature phases such as enstatite, forsterite, spinel and cordierite (**Fig. 6b**).

Three thermal mass losses for Mg^{2+}-vermiculite are 1) joint removal of physically adsorbed water as well as the first hydration sphere of interlayer cations at < 170 ℃, 2) the loss of remaining bound water associated with interlayer cations at ~180-250 ℃, and 3) dehydroxylation of vermiculite between ~650-950 °C [72].

At ~450-750 ℃, researchers found an ~8.5 times and a 20% dimensional increase with flake and compressed powder samples, respectively (**Fig. 3f**) [14, 73], explained by the escape of gas from the interlayer between vermiculite/mica or vermiculite/chlorite, rather than from vermiculite/vermiculite [74]. At higher temperatures, the first shrinkage occurs at 750-910 ℃, resulting from the dehydroxylation of vermiculite and crystallization of enstatite. A further rapid shrinkage after 910 ℃ can be ascribed to the melting of the vermiculite skeleton with liquid phase formation [14].

3.2.4. Smectite

The smectite group comprises expandable clay minerals with a common 2:1 structure (**Fig. 2e**). Three typical members of the smectite group are beidellite, nontronite and montmorillonite [75]. The ideal half-cell chemical formula for montmorillonite is $M_{0.33}$, $H_2OAl_{1.67}(Fe^{2+}, Mg^{2+})_{0.33}$ $Si_4O_{10}(OH)_2$, where M refers to a metal cation in the interlayer space between the T-O-T sheets [76].

Smectite clays are not used in large volumes as raw materials for brick manufacture because their high plasticity requires the addition of more water for kneading. This requirement can increase the potential for cracking during subsequent drying processes. Nevertheless, small amounts of low-iron smectites can be used to impart strength and give desired vitrification or color properties to bricks [77]. For the smectite group, montmorillonite is the most common in nature, and in this review, only the thermal behavior of this mineral is considered.

According to Castellini, et al. [78], the most significant feature of Ca-montmorillonite under high temperatures is the loss of vast amounts of water molecules (15.41 wt.%), with three DTG peaks occurring at 83 ℃ (the elimination of physically adsorbed water), 154 ℃ (the removal of water molecules coordinated to exchangeable cations) and 699 ℃ (dehydroxylation). Montmorillonite particles became a network of intertwined convoluted rods at 800 ℃, which stuck together at 900 ℃ due to the generation of a silica-rich melt [21]. Spinel, hematite and ilmenite appear at 800-900 ℃, while mullite is formed at 1100 ℃. Mullite forms as larger sized grains from montmorillonite (>10 μm long and 2 μm wide) than from kaolinite (1 μm x 150 nm). The presence of Ca in some montmorillonites resulted in the formation of anorthite after heating.

In addition, the thermal expansion/shrinkage of montmorillonite are: 1) a shrinkage at 150-180 ℃ due to the loss of adsorbed water, 2) a slight expansion between 700-850 ℃ due to dehydroxylation, 3) a sharp shrinkage between 900 ℃ and 1150 ℃ caused by the destruction of montmorillonite structure and crystallization of a few phases like mullite and cristobalite/opal-CT, and 4) another shrinkage at 1250-1400 ℃ resulting from melting (vitrification) of the Ca-rich system at a higher melting temperature (**Fig. 3g**).

3.2.5. Chlorite

The structure of chlorite is different from other 2:1 clay minerals. Two separate octahedral sheets are present in the unit cell: one is sandwiched between two tetrahedral sheets (2:1 layer), and the other occurs in the interlayer (**Fig. 2f**). The general formula for chlorite is: $(R_2^{2+}R^{3+})_3(OH)_6(Si_3Al)R_3^{2+}O_{10}(OH)_2$, where R^{2+} is Mg^{2+}, Fe^{2+}, Mn^{2+}, and Ni^{2+} and R^{3+} is Al^{3+}, Fe^{3+}, Cr^{3+}, and (R^{4+}) Ti^{4+} [79]. Chlorite takes part in brick production as a coincidental constituent. The thermal behavior of chlorite includes:

1) oxidation of Fe^{2+} to Fe^{3+}

$$Fe^{2+} + OH^{-} \rightarrow Fe^{3+} + O^{2-} + H\bullet \qquad (12)$$

where 2H• radicals form H_2, so this process is also denoted as “dehydrogenation” [79].

2) dehydroxylation

Chlorite dehydroxylates between 400 and 850 °C [79]. The interlayer octahedral sheets always dehydroxylate at a lower temperature (~550 ℃) than that of the 2:1 layer (~800 ℃) [80]. A theoretical ratio of the mass losses resulting from these two processes is 3:1 [79].

3) decomposition and recrystallization

Chlorite decomposes at around 700-850 ℃ to form high-temperature phases such as spinel, enstatite, hematite, and olivine/forsterite, depending on the initial chemical composition [80, 81]. An ideal reaction based on calcination of a theoretical Fe-clinochlore is as follows [81]:

$$2[MgFeAl(O)_{2.5}(O)][(Si_3Al)Mg_2FeO_{10}(O)_{0.5}(O)](Fe-clinoclore) \rightarrow 2MgSiO_3(enstatite) + 2MgAl_2O_4(spinel) + 2MgFe_2O_4(spinel) + 4SiO_2(amorphous) \qquad (13)$$

3.2.6. Sepiolite and palygorskite

Palygorskite (also known as attapulgite) and sepiolite are two fibrous clay minerals with close structural and chemical characteristics. Considering their similar thermal behaviors, only palgorskite is discussed below. Palygorskite with an ideal formula of $(OH_2)_4(Mg, Al, Fe,)_5(OH)\cdot 2Si_8O_{20}\cdot 4H_2O$ is a hydrous layered magnesium- and aluminium-rich silicate clay mineral that usually occurs as fine-grained or poorly crystalline masses [82]. The structure of palygorskite contains ribbons of 2:1 phyllosilicate layers made of linked double silicate chains that are sandwiched by Mg, Al, Fe-(O, OH) octahedral strips (**Fig. 2g**).

Playgorskite is rarely found in raw materials for brick manufacturing. Upon heating, different mass loss steps are commonly identified on TGA curves for palygorskite below 1000 ℃. Huang, et al. [83] observed five mass loss steps corresponding to DTG peaks at 58 ℃, 94 ℃, 223 ℃, 383 ℃ and 471 ℃. The first two mass losses overlap, representing the elimination of hygroscopic and zeolitic water. DTG peaks at 223 ℃ and 383 ℃ are attributed to the loss of the first part and residual coordinated water, respectively. Hydroxyl groups are relatively stable so they evaporate at 471 ℃. At around 800-900 ℃, the characteristic (110) reflection of palygorskite is hardly detectable on an XRD pattern [84]. Furthermore, the morphologic evolution of palygorskite at high temperatures differs. Chen, et al. [85] demonstrated that palygorskite fibers contract and bend at 1000 °C to form an "earthworm" appearance, consistent with a result described by Wang, et al. [84]. However, Boudriche, et al. [86] reported melt and disappearance of palygorskite fibers at 1000 °C. In addition, Zhang, et al. [87] found remnants of palygorskite fibers at 1240 °C, different to the above conclusions, although relevant EDS data have not been provided for further confirmation. Recent research by Wang, et al. [9] revealed a diminished fibrous morphology of palygorskite accompanied by the formation of larger-sized acicular cordierite particles at 1150 ℃. These cordierite particles can lead to the high mechanical strength of fired bricks due to fiber reinforcement. Wang, et al. [9] also conducted a TD analysis on the palygorskite sample (**Fig. 3h**). Their result shows four steps of dimensional change for palygorskite between 25-1150 ℃, which are: 1) a constant length below 300 ℃, 2) a 1.13% length decrease between 300-500 ℃, caused by folding of the palygorskite structure, 3) a 11.25% shrinkage at 500-820 ℃ related to the dehydroxylation and decomposition of palygorskite, and 4) a shrinkage in a small temperature interval after 890 ℃ due to melting of palygorskite.

4. Effects of clay minerals on raw material and product properties

The physical, mechanical and thermal conductivity/diffusivity properties are three key aspects of fired clay brick products. As the major component in the raw material for brick making, the effects of clay minerals on these properties are reviewed in this section. In addition, publications on other ceramic products are also considered because of similar firing regimes and practices. As the plasticity of brick raw materials endowed by clay minerals inside is critical for brick shaping or molding, it is also discussed in this section.

4.1. Physical properties

4.1.1. Plasticity

The plasticity of clays is related to the morphology of the plate-like clay mineral particles that slide over the others when water is added, which acts as a lubricant [88]. The variations of clay minerals, both in content and type, decisively affect the plasticity of clayey raw materials for brick production. Typically, higher clay mineral concentrations result in larger plastic and liquid limit values, which means more water and/or force is required to shape materials to a brick format [88]. However, this is not always true since the plasticity is also influenced by characteristics of clay minerals, such as genesis, degree of crystallinity, microstructure, initial moisture content, particle size distribution, type of exchangeable cations and impurities [89]. The plasticity of different clay minerals can be estimated using a typical clay-water-quartz system as shown for a montmorillonite-quartz mixture:

$$Liquid\ limit(wt\%) = 5.057 \times Clay\ mineral\ fraction\ (wt\%),$$

Similarly, for a kaolinite-quartz mixture, as well as an illite-quartz mixture: $Liquid\ limit(wt\%) = 0.822 \times Clay\ mineral\ fraction\ (wt\%)$ [90].

Montmorillonite exhibits higher plasticity than kaolinite and illite, attributed to exchangeable cations in the interlayer spacing, which can absorb multiple layers of water molecules. A similar phenomenon has also been identified by Dumbleton and West [91]. These authors also confirmed the effect of clay mineral genesis and structure on plastic performance. For example, they found that soils from Kenya containing disordered kaolinite exhibit higher plastic and liquid limits than soils containing more well-ordered kaolinites, which are of hydrothermal origin.

Skempton [92] and Mitchell and Soga [93] broadened the investigation of plasticity to other types of clay minerals including palygorskite, halloysite and muscovite, as well as non-clay phases such as calcite and quartz. They defined the "plastic activity" of a clay mineral as:

$A = Plasticity\ index \div Clay\ mineral\ fraction(\%)$,

where the clay mineral fraction is usually taken as the weight percentage of clay minerals in soil materials. Since the plasticity index determines two parameters which are the amount and type of clay minerals, the defined plastic activity can be used to evaluate clay mineral types. A ranking of "plastic activity" for common phases in soils is as follow: Na-montmorillonite (4-7) > Ca-montmorillonite (1.5) > illite (0.5-1.3) ≈ palygorskite = allophane (0.5-1.2) > halloysite (dehydrated) (0.5) > kaolinite (0.3-0.5) > muscovite = calcite (0.2) > halloysite (hydrated) (0.1) > quartz (0). This cascade of mineral behaviors is similar to a chart proposed to identify clay minerals using both plasticity index and plastic limit as parameters [94].

According to these studies, it may be inappropriate to simply declare a positive correlation between plasticity index and clay mineral content in soils, although it may be generally true. The published plasticity values of clay minerals are for reference only because clay minerals in real cases may differ from those in the literature, and because natural soils usually contain more than one type of clay mineral. The crystallinity, grain size and interlayer ions can significantly influence the plasticity index value, even for the same type of clay mineral. For example, K^+-montmorillonite exhibits only around 1/5 of the plasticity index of Na^+-montmorillonite due to a low hydration ability [94]. What makes characterisation more complex is that non-clay mineral components may also induce plasticity, such as organic matter or iron oxides, when they occur as clay-sized particles. Thus, these constituents have to be taken into account during the plasticity test. In brief, the clayey materials applied to make bricks should have a plasticity index value ranging from 7 to 15, as higher plasticity index values generally cause considerable linear drying shrinkage, increasing the possibility of cracking or internal fractures [95].

4.1.2. Firing shrinkage

Firing shrinkage from dry to fired brick body is another crucial parameter for brick production resulting from particle densification upon heating. This parameter can be used as a comparative indicator of the degree of vitrification as these two features usually positively correlate [96]. Low firing shrinkages generally lead to high porosity and thus low strength, while a high shrinkage increases the risk of deformation [97]. Usually, a good quality brick exhibits a firing shrinkage below 8% [98].

Clay minerals can affect firing shrinkage both positively and negatively depending on different thermal behaviors. Positive effects include dehydration of physically absorbed water, dehydroxylation of 1:1 type clay minerals (kaolinite and halloysite), the collapse of clay mineral structure at high temperature, solid-state sintering, and segregation of silicon-rich liquid phase(s). Negative effects are related to expanded crystalline volume with temperature, dehydroxylation of 2:1 type clay minerals as mentioned above, and exfoliation of specific clay minerals such as vermiculite. In addition, cations such as K^+, Na^+, Fe^{2+}, Fe^{3+}, Ca^{2+} and Mg^{2+}, in natural clay minerals (illite/muscovite, chlorite, vermiculite, sepiolite and montmorillonite) through isomorphism or interlayer bonding, can act as a fluxing agent to promote liquid-state sintering and through this, exaggerate the effects of firing shrinkage.

Although nearly all types of clay minerals compact rapidly at above 900-1000 ℃, improving the concentrations of certain clay minerals will not always result in a larger firing shrinkage in an actual situation. The final result is mainly dependent on 1) the adopted firing temperature and heating rate and 2) the residual components (quartz, feldspar, carbonates, Fe or Al hydroxides and other types of clay minerals) in the starting material.

In relation to the effect of temperature, Sallam, et al. [99] reported an increase in firing shrinkage with talc content at 1150 ℃ and 1200 ℃, but a reverse situation was observed when the temperature reached 1300 ℃. Similar phenomena were also identified by Mukhopadhyay et al. [15, 100] using pyrophyllite to replace china clay or quartz by 0-15 wt.% and 0-25 wt.%, respectively. The firing shrinkage increased at 1150 ℃ and 1200 ℃ and reduced at 1250 ℃ and 1300 ℃. The larger firing shrinkage was caused by the K^+ and Na^+ from pyrophyllite which resulted in better vitrification at lower temperatures but the subsequent drop at higher temperatures was not interpreted by these authors. Apart from talc and pyrophyllite, illite may be another promising fluxing agent which can replace feldspar and provide a larger firing shrinkage over a relatively wide temperature range of 900-1250 ℃ [16].

Notably, the pursuit of firing shrinkage can be fickle when the original clay mineral(s) in the raw material are replaced by another. For example, Barreto and da Costa [101] identified a rising to declining firing shrinkage trend with an increased concentration of illite clay in the kaolinite-based raw material after 1100 ℃ firing. Wu, et al. [102] found that adding talc to a mix of graphite tailings, kaolin, shale, potash feldspar and albite did not result in a large difference in the firing shrinkage at 1040 ℃. In addition, Wang et al. [9, 14] reported that vermiculite and palygorskite could increase the firing shrinkage of the 1150 ℃ fired kaolinite/illite-rich clay mixture. Published data on the effects of clay minerals on the firing shrinkage of the brick/ceramic body are summarized in **Table 2**.

Table 2. Effects of clay minerals on the firing shrinkage of brick/ceramic materials.

Clay or clay mineral add	Phases replaced	Temp (℃)	Firing shrinkage	Reference
Bentonite (0-10 wt.%)	kaolin, grog (crushed brick aggregate), feldspar and flint	1100	increased by 33%	[103]
Bentonite (0-15 wt.%)	feldspar	1200	increased by 32%	[17]
Kaolinite (25-75 wt.%)	waste serpentine	1100-1300	increased at 1100 ℃ and 1200 ℃, while decreased at 1150 ℃, 1250 ℃ and 1300 ℃	[52]
Illite (25 wt.%)	microcline	900-1300	increased by ~21% at 1250 ℃	[16]
Illite clay (30 wt.%)	sand and industrial body campos	850-1100	increased by ~142% at 1100 ℃	[104]
Illite clay	kaolinite clay	950 and 1100	decreased by ~69% at 950 ℃, while increased then dropped at 1100 ℃	[101]
Playgorskite (0-50 wt.%)	kaolinite-illite clay mix	1150	increased by 262%	[9]
Pyrophyllite (20-40 wt.%)	Suzhou clay	1250-1400	irregularly changed	[105]
Pyrophyllite (0-15 wt.%)	China clay	1150-1300	increased at 1150 ℃ and 1200 ℃, while decreased at 1200 ℃ and 1250 ℃	[15]
Pyrophyllite (0-25 wt.%)	quartz	1150-1300	increased at 1150 ℃ and 1200 ℃, while decreased at 1200 ℃ and 1250 ℃	[100]
Pyrophyllite (15 wt.%)	quartz	1150-1300	increased at 1150 ℃ and 1200 ℃, while decreased at 1250 ℃ and 1300 ℃	[106]
Talc (0-8 wt.%)	feldspar	1230	increased by ~11.1% from 0 to 4 wt.% talc, then stabled at 4-8 wt.% talc	[107]
Talc (3 wt.%)	feldspar	1120-1180	increased by 24%, 22% and 7% at 1120 ℃, 1140 ℃ and 1160 ℃, respectively, then stabilized at 1180 ℃	[19]
Talc (5-15 wt.%)	quartz	1230-1300	increased at 1150 -1225 ℃, while decrease at 1300 ℃	[99]
Talc (0-6 wt.%)	kaolinite clay, illite clay, sand and feldspar	1050-1250	increased at 1050-1200 ℃, while decreased at 1225 ℃ and 1250 ℃	[108]
Talc (0-16.67 wt.%)	graphite tailings, kaolin, shale and feldspar	1040-1120	irregularly changed	[102]
Vermiculite (16.5 wt.%)	red clay	1060	increased by 46%	[109]
Vermiculite (0-30 wt.%)	kaolinite-illite clay mix	1150	increased by 101%	[14]

Note: Some variations in the firing shrinkage were not shown in the original literature and are calculated by the authors.

4.1.3. Porosity

Porosity refers to the volumetric ratio of empty spaces in fired clay bricks. This parameter is a vital characteristic affecting the mechanical strength, durability and thermal conductivity of brick products [110]. The porosity of brick is significantly dependent on the mineralogical composition of the initial clay mix and firing regime [111].

As expected, clay minerals significantly affect the porosity of fired bricks, but the relationship between clay type and porosity is enigmatic due to inadequate research and lack of critical information in the literature, such as starting material purity, crystallinity, chemistry and grain size of clay minerals. One can infer that increasing clay mineral content (excluding vermiculite) at the expense of non-clay ingredients may result in reduced porosity above 950 °C. Relevant research that describes this inference includes the use of bentonite to replace fly ash and red mud [112], bentonite to replace feldspar [17], illite to replace feldspar [16], talc to replace quartz [99], and pyrophyllite to replace quartz [106]. The possible reasons for this trend are as follows: 1) clay minerals have finer particle sizes than non-clay constituents and thus, the porosity of the green body is lower when containing more clay minerals, 2) abundant cations in clay minerals can act as fluxing promoters to enhance the vitrification process, 3) the common existence of Al in clay minerals generates acicular mullite at high temperature resulting in an interlocked structure, and 4) the Si in clay mineral melts to form liquid phases containing K, Na, Mg, etc. which can reduce open porosity.

It should be noted that much of the research mentioned above focused on apparent porosity which involves open pores (permeability). Closed porosity is not well characterized because of the limited use of adequate techniques. Two feasible approaches to determine closed pores are micro-CT and pycnometer. The latter technique compares brick densities before and after reducing particle sizes to below 53 μm [113]. Some scholars report increased closed porosity/total porosity due to more clay minerals (contrary to what was reported above) [19, 108, 114]. The possible reason is that more liquid/vapour phases are generated, transforming connected pores into closed ovoid ones due to surface tension. Wang, et al. [9] observed the formation of closed pores from interconnected irregular pores in clay bricks fired at 1150 ℃. In addition, porosity may be unpredictable when a well-characterized clay mineral mix in the starting material is substituted by other types. For instance, Mukhopadhyay, et al. [15] used pyrophyllite to replace china clay and obtained decreasing apparent porosity from 1150-1300 ℃. Wu, et al. [102] used talc to replace kaolinite clay but the apparent porosity (as determined by conversion of tested water absorption values) remained unchanged. In particular, vermiculite is a special clay mineral worthy of further attention because of its expansion property and porous structure. Some scholars demonstrated a higher porosity of brick fired at 900-1000 ℃ after adding expanded vermiculite [18, 115], while smaller apparent porosity was obtained after firing with 5% raw vermiculite addition at 1150 ℃ [14].

4.1.4. Color

In the brick industry, the color of the finished product is a fundamental property. Indeed, from a commercial point of view it may be the most important feature because many architects and consumers select bricks based on aesthetic considerations [116]. So far, few investigations are reported in the literature on the firing color of clay brick products, particularly the effect of clay minerals on color development. However, principal factors such as the firing temperature, atmosphere and metallic elements (especially transition metals) in the starting material are considered essential to the determination of the final obtained colors [117].

Common metallic elements in natural clayey materials include Al, Fe, Ca, Na, K, Mg, Ti, Zr and Mn. Among them, Fe is undoubtedly the most striking which provides α-Fe_2O_3 under oxidizing firing conditions that induces a reddish color [118]. The concentration of Fe also matters as mentioned by Clifford [116] - less than 1 wt.% Fe (as oxide) brings white, while 1-

2 wt.% imparts a yellow color; 2-3 wt.% produces buff and 4-5 wt.% and above gives red. Exceptions occur if some high-temperature crystalline components (e.g., mullite, gehlenite and pyroxene) incorporate Fe into their structures, resulting in a reduced amount of formed hematite. This effect will also change the color of the fired phases. For example, mullite varies from cream to buff depending on the Fe content [116]. Apart from Fe, other metallic elements affect brick colors in different formats. Normally, Ca brings buff to yellow colors due to the formation of calcium silicates or calcium ferrite spinel; Mn gives a dark color; Mg results in a willow-green color and Ti may endow a blue color. Alkali metal elements such as K and Na affect the brick color by enhancing the formation of melts thus changing the final mineralogical form of Fe [118].

Clay minerals can change the color of bricks by accommodating the above cations in their structures. Clifford [116] reported that Fe could derive from illite to produce red bricks. Wang et al. [9, 14] observed Mg and Fe in palygorskite and vermiculite induced a black olive color at 1150 °C. Although kaolinite and halloysite are comprised primarily of Si and Al, which do not determine the color of fired clays, influence is there. A coloring agent, such as Fe, can dissolve in kaolinite/halloysite reaction products, so the obtained red color is diluted because less hematite is formed.

4.2. Mechanical properties

The mechanical strengths of fired brick materials, involving compressive strength, flexural strength and tensile strength, have been extensively reported [119-122]. Compressive strength is the major performance criteria for fired bricks as these construction materials mostly experience compressive loads, while flexural strength and tensile strength are more frequently tested on porcelain samples.

The effect of clay minerals on the mechanical strength of fired bricks is similar to that on porosity, as reviewed in Section 4.1.3. This similarity is because mechanical strength and porosity are commonly positively correlated. In most cases, an increased amount of clay minerals in brick making raw material, at the expense of non-clay phases, improves mechanical strength. Published research on this topic has been summarized in **Table 3**, with underlying mechanisms described in Section 4.1.3. Exceptions may occur if excessive clay minerals are added to an initial mix or if the raw material is overfired. These exceptions are confirmed by experiment, using talc and pyrophyllite to replace feldspar and quartz, respectively [19, 100]. A higher proportion of clay minerals or higher firing temperature can generate excessive liquid phases in the brick body which results in more deformation during firing. Thus, the final strength is lower than that for lower proportions or firing temperatures.

Table 3. Effects of clay minerals on the mechanical strength of brick/ceramic materials.

Clay/clay minerals added	Phases replaced	Fired Temp (ºC)	Mechanical strength	Reference
Ca bentonite (0-15 wt.%)	feldspar	1000-1400 ℃	flexural strength increased at 5-10 wt.% addition and decreased at 15 wt.% addition; strength increased by ~63% at 10 wt.% addition, 1375 ℃	[114]
Bentonite (0-10 wt.%)	kaolin, grog, feldspar and flint	1100 ℃	flexural strength increased by 39%	[103]
Bentonite (0-15 wt.%)	feldspar	1200 ℃	flexural strength increased by 16%	[17]
Bentonite (0-10 wt.%)	fly ash and red mud	1150 ℃	flexural strength increased by ~80%	[112]
Kaolinite rich clay (0-30 wt.%)	red-firing clay	1000 ℃	flexural strength almost unchanged	[123]
Illite (25 wt.%)	microcline	1100-1300 ℃	flexural strength increased by ~123% at 1250 ℃	[16]
Illite clay (30 wt.%)	sand and industrial body campos	850-1100 ℃	flexural strength increased by ~204% at 1100 ℃	[104]
Palygorskite (0-50 wt.%)	kaolinite-illite clay mix	1150 ℃	compressive strength increased by 70%	[9]
Pyrophyllite (20-40 wt.%)	Suzhou clay	1250-1400 ℃	cold crushing strength decreased by ~46% at 1400 ℃	[105]
Pyrophyllite (0-15 wt.%)	China clay	1150-1300 ℃	flexural strength increased at 1150 ℃ and 1200 ℃, but first increased then decreased at 1250 ℃ and 1300 ℃	[15]
Pyrophyllite (0-25 wt.%)	quartz	1150-1300 ℃	flexural strength increased at 1150 ℃, but first increased then decreased at 1200 ℃, 1250 ℃ and 1300 ℃	[100]

Pyrophyllite (15 wt.%)	quartz	1150-1300 ℃	flexural strength increased by ~40% at 1250 ℃	[106]
Talc (0-8 wt.%)	feldspar	1230 ℃	flexural strength increased by ~21% at 5 wt.% addition	[107]
Talc (3 wt.%)	feldspar	1120-1180 ℃	flexural strength increased by ~15% and at 1120 ℃ and 1140 ℃, while decreased by 12% and 19% at 1160 ℃ and 1180 ℃, respectively	[19]
Talc (5-15 wt.%)	quartz	1230-1300 ℃	Tensile strength increased	[99]
Talc (0-16.67 wt.%)	graphite tailings, kaolin, shale and feldspar	1040-1120 ℃	flexural strength irregularly changed	[102]
Expanded vermiculite (0-10 wt.%)	illite and chlorite clay	900-1000 ℃	compressive strength decreased	[115]
Expanded vermiculite (0-25 wt.%)	water treatment sludge	1000 ℃	compressive strength decreased by 75%	[18]
Vermiculite (0-30 wt.%)	kaolinite-illite clay mix	1150 ℃	compressive strength increased by 22% at 5 wt.% addition while decreased by 41% at 30 wt.% addition	[14]

Note: Some variations in the mechanical strength are calculated and summarized by authors; these values may not be shown directly in the original literature.

The mechanical strength can also change if the original clay/clay mineral in the starting material is replaced by another clay/clay mineral (**Table 3**). However, it is difficult to make an accurate prediction if information, such as the particle size, purity, structure and composition of these clays/clay minerals, is not available; this is usually true in many early studies. A comprehensive database covering the above parameters as input variables may be a promising development that enables an accurate forecast of effects on strength changes in brick manufacture. Arsenovic, et al. [124] have developed simple artificial neural network-based models to predict the compressive strength of bricks based on the chemical content of raw materials and firing temperature. Their work may be a useful benchmark for further investigations on the effect of clay minerals on brick properties.

4.3. Thermal conductivity/diffusivity

Compared to physical and mechanical properties, the thermal conductivity/diffusivity properties of fired clay bricks have garnered limited attention. However, the importance of thermal conductivity/diffusivity has been increasingly recognized in recent years due to worldwide concerns about energy saving [125]. Since around one-third of the energy in the world is consumed in buildings for thermal conditioning, an essential way to achieve better energy efficiency is to improve the thermal insulation properties of building envelopes [115]. Generally, the thermal conductivity of fired bricks is governed by the bulk density. Ten, et al. [126] identified a linear relationship between bulk density and thermal conductivity when firing an illite-kaolinite clay. However, a more comprehensive comparison covering hundreds of samples indicates that the correlation between thermal conductivity and bulk density is not statistically significant since comprehensive data analysis shown in **Fig. 7a** exhibits a broad scatter around a linear trend. In fact, a few scholars have found that thermal conductivity is also affected by the nature of the pore system, the mineralogical composition and the microstructure of brick products [123, 125].

As the most crucial raw material for brick manufacturing, clay minerals can, of course, change the bulk density, porosity, composition and structure of brick products, and through this, significantly affect thermal conductivity/diffusivity. So far, the correlation between clay minerals and thermal conductivity/diffusivity has received limited study. Gualtieri, et al. [125] reported that thermal conductivity might not be positively correlated with total clay mineral content in the raw material because the type and features of clay minerals also matter (**Fig. 7b**). In addition, among all clay minerals, vermiculite is the one that has been chiefly reported for its impact on brick thermal conductivity/diffusivity properties. Expanded vermiculite can act as a pore-forming agent which produces lightweight thermal insulation bricks (**Fig. 7c**). Wang, et al. [14] concluded that the firing temperature is crucial to determine the thermal behavior of vermiculite. When 1150 °C was used, an increase in thermal diffusivity of vermiculite-added bricks was observed instead of a decrease (**Fig. 7d**). A possible reason is the fluxing action of vermiculite when the temperature is raised which can densify the brick body, and so reduced porosity is obtained.

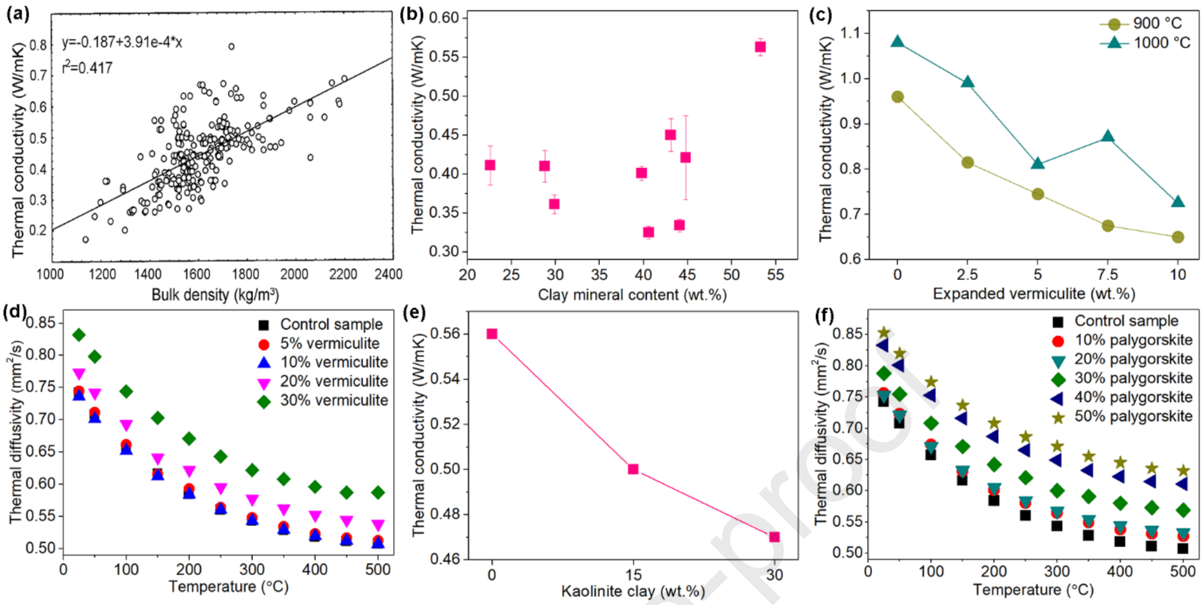

Fig. 7. (**a**) Thermal conductivity versus bulk density values [8]; (**b**) Thermal conductivity versus the clay mineral content in the raw material; the clay mineral types also change at different points [125]; (**c**) Thermal conductivity versus expanded vermiculite added [18]; (**d**) Thermal diffusivity versus vermiculite added [14]; (**e**) Thermal diffusivity versus kaolinite clay added [123]; (**f**) Thermal diffusivity versus palygorskite added [9]. (**a**)-(**f**) are reproduced with permission.

Apart from vermiculite, the effects of other clay minerals on thermal conductivity/diffusivity are only rarely mentioned. For example, kaolinite-rich clay may result in a lower thermal conductivity than an illite-rich clay (**Fig. 7e**). Palygorskite leads to higher thermal diffusivity when added to kaolinite-illite clay (**Fig. 7f**). However, studies on this subject are still insufficient to draw definitive conclusions.

5. Conclusions

By drawing on research experience from building materials, mineralogy, and porcelain/earthenware materials, the relationship between raw materials and fired brick properties is provided in this review. Progress on two aspects (a) thermal behaviors of clay minerals and (b) the effects of clay minerals on brick properties, have been reviewed. Key conclusions are:

1) Typical thermal behaviors of clay minerals in brick manufacture

Thermal behaviors of natural clay minerals used in brick manufacture, including phase transformation, mass loss, shrinkage/expansion, and morphological change, have been presented. Under firing, the structural evolution of clay minerals can be divided into four steps, including dehydration, dehydroxylation, decomposition, and crystallization of new phases.

2) Effects of inherent and acquired features

The thermal behavior and final phases obtained from clay minerals are significantly affected by inherent and acquired features. Inherent features refer to geological genesis that often determines the crystallinity, purity, morphology and chemistry of a clay mineral [127]. Parent rocks and geological settings are two crucial aspects determining geological genesis. Acquired features include artificial crushing and grinding before the molding process which changes the particle size and crystallinity [128].

3) Importance of clay mineral characterization

During industrial brick production, higher precision and reproducibility may be afforded by quality mineralogical characterization rather than the use of simple definitions for clays as fractions with particle sizes less than 2 μm. A better understanding of raw materials (including clay minerals) will clearly reduce the proportion of brick manufacture failure.

4) Influence of substituted and absorbed metal ions

The alkali and alkaline earth elements in clay minerals, including K, Na, Ca, Mg and Fe, play a vital role in the physical, mechanical and thermal conductivity/diffusivity properties of fired bricks. These elements can act as fluxing agents to create lower porosity, higher firing shrinkage, mechanical strength and thermal conductivity, as well as change the color of fired bricks.

5) Firing regime and associated phases

Besides their own features, the effects of clay minerals on brick properties also depend on the firing regime, the concentration of clay minerals, and the component of residual phases in the starting material.

6. Outlooks

In order to economically develop higher-quality brick products with lower reject rates, a better understanding of raw clayey materials and their influence on brick manufacturing is required. A few *in-situ* techniques such as *in-situ* temperature controllable XRD as mentioned in this review may enable a higher level of detail and understanding of reactions that have not been available previously. Combinations of techniques such as *in-situ* XRD, TGA and TD in the future may provide adequate real-time monitoring data for brick production and research. Additionally, key information on some brick-forming clay minerals is limited and may lead to misinterpretation of early studies. In future work, we advocate the provision of more detailed information from a clay science perspective such as geological origin, crystallinity, morphology, quantitative mineralogical and chemical compositions. A consistent approach to clay characterization may identify a quantitative relationship or model to predict the effects of clay minerals on all properties of fired bricks.

Acknowledgements

This work is funded by an Advance Queensland Research Fellowship project (Grant No. AQRF01716-17RD2), Brickworks Ltd., the Centre for Clean Energy Technologies and Practices, and the Central Analytical Research Facility (CARF), QUT.

References

[1] R.E. Grim, Clay mineralogy, Science 135 (3507) (1962) 890-898, 10.1126/science.135.3507.890.

[2] F. Bergaya, G. Lagaly, Handbook of Clay Science, second ed., Elsevier, 2013.

[3] R.A. Schoonheydt, Reflections on the material science of clay minerals, Appl. Clay Sci. 131 (2016) 107-112, 10.1016/j.clay.2015.12.005.

[4] A. Mohajerani, A. Ukwatta, T. Jeffrey-Bailey, M. Swaney, M. Ahmed, G. Rodwell, S. Bartolo, N. Eshtiaghi, S. Setunge, A Proposal for Recycling the World's Unused Stockpiles of Treated Wastewater Sludge (Biosolids) in Fired-Clay Bricks, Buildings 9 (1) (2019) 14, 10.3390/buildings9010014.

[5] J.Z. Sun, H. Zhou, H.H. Jiang, W.Y. Zhang, L.Q. Mao, Recycling municipal solid waste incineration fly ash in fired bricks: An evaluation of physical-mechanical and environmental properties, Constr. Build. Mater. 294 (2021) 123476, 10.1016/j.conbuildmat.2021.123476.

[6] G. Cultrone, F.J.C. Rosua, Growth of metastable phases during brick firing: Mineralogical and microtextural changes induced by the composition of the raw material and the presence of additives, Appl. Clay Sci. 185 (2020) 105419, 10.1016/j.clay.2019.105419.

[7] A. Zaccaron, V.D. Nandi, A.M. Bernardin, Fast drying for the manufacturing of clay ceramics using natural clays, J. Build. Eng. 33 (2021), 10.1016/j.jobe.2020.101877.

[8] M. Dondi, F. Mazzanti, P. Principi, M. Raimondo, G. Zanarini, Thermal conductivity of clay bricks, J. Mater. Civ. Eng. 16 (1) (2004) 8-14, 10.1061/(Asce)0899-1561(2004)16:1(8).

[9] S. Wang, L. Gainey, X. Wang, I.D. Mackinnon, Y. Xi, Influence of palygorskite on in-situ thermal behaviours of clay mixtures and properties of fired bricks, Appl. Clay Sci. 216 (2022) 106384, 10.1016/j.clay.2021.106384.

[10] M. Dondi, B. Gian Paolo, Basic Guidelines for Prospecting and Technological Assessment of Clays for the Ceramic Industry. Part 2, InterCeram: Int. Ceram. Rev. 71 (1) (2022) 28-37.

[11] L.Y. Zhang, Production of bricks from waste materials - A review, Constr. Build. Mater. 47 (2013) 643-655, 10.1016/j.conbuildmat.2013.05.043.

[12] G. El Boukili, M. Lechheb, M. Ouakarrouch, A. Dekayir, F. Kifani-Sahban, A. Khaldoun, Mineralogical, physico-chemical and technological characterization of clay from Bensmim (Morocco): Suitability for building application, Constr. Build. Mater. 280 (2021) 122300, 10.1016/j.conbuildmat.2021.122300.

[13] D. Tsozue, A.N. Nzeugang, J.R. Mache, S. Loweh, N. Fagel, Mineralogical, physico-chemical and technological characterization of clays from Maroua (Far-North, Cameroon) for use in ceramic bricks production, J. Build. Eng. 11 (2017) 17-24, 10.1016/j.jobe.2017.03.008.

[14] S. Wang, L. Gainey, J. Marinelli, B. Deer, X. Wang, I.D. Mackinnon, Y. Xi, Effects of vermiculite on in-situ thermal behaviour, microstructure, physical and mechanical properties of fired clay bricks, Constr. Build. Mater. 316 (2022) 125828, 10.1016/j.conbuildmat.2021.125828.

[15] T.K. Mukhopadhyay, S. Ghatak, H.S. Maiti, Effect of pyrophyllite on the mullitization in triaxial porcelain system, Ceram. Int. 35 (4) (2009) 1493-1500, 10.1016/j.ceramint.2008.08.002.

[16] D. Wattanasiriwech, S. Wattanasiriwech, Fluxing action of illite and microcline in a triaxial porcelain body, J. Eur. Ceram. Soc. 31 (8) (2011) 1371-1376, 10.1016/j.jeurceramsoc.2011.01.025.

[17] W. Widodo, S. Solihin, S. Subari, Effect of Karangunggal bentonite addition on the mechanical strength of conventinal ceramics, Indones. Min. J. 22 (1) (2019) 19-28, 10.30556/imj.Vol22.No1.2019.962.

[18] O. Gencel, O. Kizinievic, M. Sutcu, E. Erdogmus, P.M. Velasco, D. Eliche-Quesada, V. Kizinievic, H. Kurmus, Effects of expanded vermiculite on the properties of fired bricks from

water treatment sludge, Int. J. Appl. Ceram. Technol. 19 (2022) 1214– 1226, 10.1111/ijac.13979.

[19] V. Biasini, M. Dondi, G. Guarini, M. Raimondo, A. Argnani, S. Di Primio, Effect of talc and chlorite on sintering and technological behaviour of porcelain stoneware tiles, Silic. Ind. 68 (5) (2003) 67-73.

[20] G.Y. Wang, H.J. Wang, N. Zhang, In situ high temperature X-ray diffraction study of illite, Appl. Clay Sci. 146 (2017) 254-263, 10.1016/j.clay.2017.06.006.

[21] C.J. McConville, W.E. Lee, Microstructural development on firing illite and smectite clays compared with that in kaolinite, J. Am. Ceram. Soc. 88 (8) (2005) 2267-2276, 10.1111/j.1551-2916.2005.00390.x.

[22] A.F. Gualtieri, Thermal behavior of the raw materials forming porcelain stoneware mixtures by combined optical and In situ X-ray dilatometry, J. Am. Ceram. Soc. 90 (4) (2007) 1222-1231, 10.1111/j.1551-2916.2007.01614.x.

[23] P.M. Velasco, M.P.M. Ortiz, M.A.M. Giro, L.M. Velasco, Fired clay bricks manufactured by adding wastes as sustainable construction material - A review (vol 63, pg 97, 2014), Constr. Build. Mater. 68 (2014) 783-783, 10.1016/j.conbuildmat.2014.06.023.

[24] A. Al-Fakih, B.S. Mohammed, M.S. Liew, E. Nikbakht, Incorporation of waste materials in the manufacture of masonry bricks: An update review, J. Build. Eng. 21 (2019) 37-54, 10.1016/j.jobe.2018.09.023.

[25] A.M. Sorte, A.N. Burile, A.R. Chaudhari, A. Haldar, Utilisation of agro waste in the development of fired clay bricks–a review, Int. J. Environ. Waste Manag. 26 (4) (2020) 531-550, 10.1504/IJEWM.2020.110400.

[26] R.T. Martin, S.W. Bailey, D.D. Eberl, D.S. Fanning, S. Guggenheim, H. Kodama, D.R. Pevear, J. Srodon, F.J. Wicks, Report of the Clay-Minerals-Society Nomenclature Committee

- Revised Classification of Clay Materials, Clays Clay Miner. 39 (3) (1991) 333-335, 10.1346/Ccmn.1991.0390315.

[27] P. Ptacek, M. Kreckova, F. Soukal, T. Opravil, J. Havlica, J. Brandstetr, The kinetics and mechanism of kaolin powder sintering I. The dilatometric CRH study of sinter-crystallization of mullite and cristobalite, Powder Technol. 232 (2012) 24-30, 10.1016/j.powtec.2012.07.060.

[28] Y. Tsuzuki, K. Nagasawa, A transitional stage to the 980° C exotherm of kaolin minerals, Clay Science 3 (5) (1969) 87-102, 10.11362/jcssjclayscience1960.3.87.

[29] D. Hrsak, G. Sucik, L. Lazic, The thermophysical properties of serpentinite, Metalurgija 47 (1) (2008) 29-31.

[30] T. Ondro, T. Hulan, O. Al-Shantir, S. Csaki, T. Vaclavu, A. Trnik, Kinetic analysis of the formation of high-temperature phases in an illite-based ceramic body using thermodilatometry, J. Therm. Anal. Calorim. 138 (3) (2019) 2289-2294, 10.1007/s10973-019-08781-w.

[31] P.J. Sánchezsoto, I. Sobrados, J. Sanz, J.L. Pérez-Rodríguez, 29-Si and 27-Al Magic-Angle Spinning Nuclear Magnetic Resonance Study of the Thermal Transformations of Pyrophyllite, J. Am. Ceram. Soc. 76 (12) (1993) 3024-3028, 10.1111/j.1151-2916.1993.tb06604.x.

[32] J. Jimenez-Millan, I. Abad, R. Jimenez-Espinosa, A. Yebra-Rodriguez, Assessment of solar panel waste glass in the manufacture of sepiolite based clay bricks, Mater. Lett. 218 (2018) 346-348, 10.1016/j.matlet.2018.02.049.

[33] H.H. Murray, W.D. Keller, Kaolins, kaolins, and kaolins, In: H.H. Murray, W.M. Bundy, C.C. Harvey (Eds.), Kaolin Genesis and Utilization, Clay Minerals Society, 1993.

[34] H.F. Cheng, Q.F. Liu, J. Yang, S.J. Ma, R.L. Frost, The thermal behavior of kaolinite intercalation complexes-A review, Thermochim. Acta 545 (2012) 1-13, 10.1016/j.tca.2012.04.005.

[35] F. Bergaya, P. Dion, J.F. Alcover, C. Clinard, D. Tchoubar, TEM study of kaolinite thermal decomposition by controlled-rate thermal analysis, J. Mater. Sci. 31 (19) (1996) 5069-5075, 10.1007/Bf00355907.

[36] K. MacKenzie, I. Brown, R. Meinhold, M. Bowden, Outstanding problems in the kaolinite-mullite reaction sequence investigated by 29Si and 27Al solid-state nuclear magnetic resonance: I, metakaolinite, J. Am. Ceram. Soc. 68 (6) (1985) 293-297, 10.1111/j.1151-2916.1985.tb15229.x.

[37] D. Liu, Y. Zhang, A. Zhou, E.N. Nnachi, S. Huo, Q. Zhang, The Kaolinite Crystallinity and Influence Factors of Coal-Measure Kaolinite Rock from Datong Coalfield, China, Minerals 12 (1) (2022) 54, 10.3390/min12010054.

[38] O. Castelein, B. Soulestin, J.P. Bonnet, P. Blanchart, The influence of heating rate on the thermal behaviour and mullite formation from a kaolin raw material, Ceram. Int. 27 (5) (2001) 517-522, 10.1016/S0272-8842(00)00110-3.

[39] K. Nahdi, P. Llewellyn, F. Rouquerol, J. Rouquerol, N.K. Ariguib, M.T. Ayedi, Controlled Rate Thermal Analysis of kaolinite dehydroxylation: effect of water vapour pressure on the mechanism, Thermochim. Acta 390 (1-2) (2002) 123-132, 10.1016/S0040-6031(02)00082-5.

[40] R. Hamzaoui, F. Muslim, S. Guessasma, A. Bennabi, J. Guillin, Structural and thermal behavior of proclay kaolinite using high energy ball milling process, Powder Technol. 271 (2015) 228-237, 10.1016/j.powtec.2014.11.018.

[41] A. Ghorbel, M. Fourati, J. Bouaziz, Microstructural evolution and phase transformation of different sintered Kaolins powder compacts, Mater. Chem. Phys. 112 (3) (2008) 876-885, 10.1016/j.matchemphys.2008.06.047.

[42] S. Lee, Y.J. Kim, H.S. Moon, Phase transformation sequence from kaolinite to mullite investigated by an energy-filtering transmission electron microscope, J. Am. Ceram. Soc. 82 (10) (1999) 2841-2848, 10.1111/j.1151-2916.1999.tb02165.x.

[43] A.K. Chakraborty, Phase transformation of kaolinite clay, Springer, New Delhi, India, 2014.

[44] C.Z. Liao, L.M. Zeng, K.M. Shih, Quantitative X-ray Diffraction (QXRD) analysis for revealing thermal transformations of red mud, Chemosphere 131 (2015) 171-177, 10.1016/j.chemosphere.2015.03.034.

[45] I. Allegretta, G. Eramo, D. Pinto, V. Kilikoglou, Strength of kaolinite-based ceramics: Comparison between limestone- and quartz-tempered bodies, Appl. Clay Sci. 116 (2015) 220-230, 10.1016/j.clay.2015.03.018.

[46] A. Ramezani, S.M. Emami, S. Nemat, Reuse of spent FCC catalyst, waste serpentine and kiln rollers waste for synthesis of cordierite and cordierite-mullite ceramics, J. Hazard. Mater. 338 (2017) 177-185, 10.1016/j.jhazmat.2017.05.029.

[47] F. Sahnoune, M. Chegaar, N. Saheb, P. Goeuriot, F. Valdivieso, Algerian kaolinite used for mullite formation, Appl. Clay Sci. 38 (3-4) (2008) 304-310, 10.1016/j.clay.2007.04.013.

[48] J. Temuujin, K.J.D. MacKenzie, M. Schmucker, H. Schneider, J. McManus, S. Wimperis, Phase evolution in mechanically treated mixtures of kaolinite and alumina hydrates (gibbsite and boehmite), J. Eur. Ceram. Soc. 20 (4) (2000) 413-421, 10.1016/S0955-2219(99)00188-0.

[49] K.Z. Yan, Y.X. Guo, L. Fang, L. Cui, F.Q. Cheng, T.Y. Li, Decomposition and phase transformation mechanism of kaolinite calcined with sodium carbonate, Appl. Clay Sci. 147 (2017) 90-96, 10.1016/j.clay.2017.07.010.

[50] D. Njoya, A. Elimbi, D. Fouejio, M. Hajjaji, Effects of two mixtures of kaolin-talc-bauxite and firing temperatures on the characteristics of cordierite-based ceramics, J. Build. Eng. 8 (2016) 99-106, 10.1016/j.jobe.2016.10.004.

[51] A.M.M. Soltan, H. Elshimy, F. Abd EL-Raoof, F. Fuchs, A. Koenig, A.M. Yahya, M.M. AbdelFattah, M. Serry, H. Pollmann, Microstructure and phase composition of cordierite-based co-clinker, Ceram. Int. 44 (6) (2018) 5855-5866, 10.1016/j.ceramint.2017.11.179.

[52] S.M. Emami, A. Ramezani, S. Nemat, Sintering behavior of waste serpentine from abdasht chromite mines Abdasht chromite mines and kaolin blends, Ceram. Int. 43 (17) (2017) 15189-15193, 10.1016/j.ceramint.2017.08.051.

[53] R.A. Heindl, L.E. Mong, Length changes and endothermic and exothermic effects during heating of flint and aluminous clays, J. Research Natl. Bur. Standards 23 (3) (1939) 427-442.

[54] M. Rieder, G. Cavazzini, Y.S. D'yakonov, V.A. Frank-Kamenetskii, G. Gottardi, S. Guggenheim, P.W. Koval, G. Mueller, A.M. Neiva, E.W. Radoslovich, Nomenclature of the micas, Clays Clay Miner. 46 (5) (1998) 586-595, 10.1346/CCMN.1998.0460513.

[55] E. Murad, U. Wagner, Mössbauer study of pure illite and its firing products, Hyperfine Interact. 91 (1) (1994) 685-688, 10.1007/BF02064591.

[56] D. Antal, T. Hulan, I. Stubna, M. Zaleska, A. Trnik, The influence of texture on elastic and thermophysical properties of kaolin- and illite-based ceramic bodies, Ceram. Int. 43 (2) (2017) 2730-2736, 10.1016/j.ceramint.2016.11.100.

[57] A. Khalfaoui, M. Hajjaji, A Chloritic-illitic clay from Morocco: Temperature-time-transformation and neoformation, Appl. Clay Sci. 45 (1-2) (2009) 83-89, 10.1016/j.clay.2009.03.006.

[58] D. Wattanasiriwech, K. Srijan, S. Wattanasiriwech, Vitrification of illitic clay from Malaysia, Appl. Clay Sci. 43 (1) (2009) 57-62, 10.1016/j.clay.2008.07.018.

[59] G. Cultrone, C. Rodriguez-Navarro, E. Sebastian, O. Cazalla, M.J. De La Torre, Carbonate and silicate phase reactions during ceramic firing, Eur. J. Mineral. 13 (3) (2001) 621-634, 10.1127/0935-1221/2001/0013-0621.

[60] H.H. Mao, M. Hillert, M. Selleby, B. Sundman, Thermodynamic assessment of the CaO-Al2O3-SiO2 system, J. Am. Ceram. Soc. 89 (1) (2006) 298-308, 10.1111/j.1551-2916.2005.00698.x.

[61] D. Perkins, J. Brady, Ternary Phase Diagrams: the system MgO-Al2O3-SiO2 at 1 atm. pressure. https://serc.carleton.edu/research_education/equilibria/ternary_diagrams.html, 2007.

[62] T. Hulan, I. Stubna, A. Shishkin, J. Ozolins, S. Csaki, P. Bacik, J. Fridrichova, Development of Young's modulus of natural illitic clay during the heating and cooling stages of firing, Clay Miner. 54 (3) (2019) 229-233, 10.1180/clm.2019.33.

[63] M. Knapek, T. Hulan, P. Minarik, P. Dobron, I. Stubna, J. Straska, F. Chmelik, Study of microcracking in illite-based ceramics during firing, J. Eur. Ceram. Soc. 36 (1) (2016) 221-226, 10.1016/j.jeurceramsoc.2015.09.004.

[64] M.V. Vasic, L. Pezo, J.D. Zdravkovic, Z. Backalic, Z. Radojevic, The study of thermal behavior of montmorillonite and hydromica brick clays in predicting tunnel kiln firing curve, Constr. Build. Mater. 150 (2017) 872-879, 10.1016/j.conbuildmat.2017.06.068.

[65] X.W. Liu, X.X. Liu, Y.H. Hu, Investigation of the Thermal Decomposition of Talc, Clays Clay Miner. 62 (1-2) (2014) 137-144, 10.1346/Ccmn.2014.0620206.

[66] A. Benhammou, Y. El Hafiane, A. Abourriche, Y. Abouliatim, L. Nibou, A. Yaacoubi, N. Tessier-Doyen, A. Smith, B. Tanouti, Influence of sintering temperature on the microstructural and mechanical properties of cordierite synthesized from andalusite and talc, Mater. Lett. 172 (2016) 198-201, 10.1016/j.matlet.2016.02.153.

[67] G.H. Li, J.H. Zeng, J. Luo, M.X. Liu, T. Jiang, G.Z. Qiu, Thermal transformation of pyrophyllite and alkali dissolution behavior of silicon, Appl. Clay Sci. 99 (2014) 282-288, 10.1016/j.clay.2014.07.011.

[68] P.J. Sanchezsoto, J.L. Perezrodriguez, Sem Study of Pyrophyllite High-Temperature Transformations, J. Mater. Sci. 24 (10) (1989) 3774-3778, 10.1007/Bf02385769.

[69] J. Schomburg, Thermal Investigations of Pyrophyllites, Thermochim. Acta 93 (1985) 521-524, 10.1016/0040-6031(85)85131-5.

[70] V.T. Shmuradko, F.I. Panteleenko, O.P. Reut, E.F. Panteleenko, N.V. Kirshina, Composition, structure, and property formation of heat insulation fire- and heat-reflecting materials based on vermiculite for industrial power generation, Refract. Ind. Ceram. 53 (4) (2012) 254-258, 10.1007/s11148-012-9503-5.

[71] V. Balek, J. Pérez-Rodríguez, L.a. Pérez-Maqueda, J. Šubrt, J. Poyato, Thermal behaviour of ground vermiculite, J. Therm. Anal. Calorim. 88 (3) (2007) 819-823, 10.1007/s10973-005-7462-5.

[72] L.Y. Ma, X.L. Su, Y.F. Xi, J.M. Wei, X.L. Liang, J.X. Zhu, H.P. He, The structural change of vermiculite during dehydration processes: A real-time in-situ XRD method, Appl. Clay Sci. 183 (2019) 105332, 10.1016/j.clay.2019.105332.

[73] H.F. Muiambo, W.W. Focke, M. Atanasova, I. van der Westhuizen, L.R. Tiedt, Thermal properties of sodium-exchanged palabora vermiculite, Appl. Clay Sci. 50 (1) (2010) 51-57, 10.1016/j.clay.2010.06.023.

[74] S. Hillier, E.M.M. Marwa, C.M. Rice, On the mechanism of exfoliation of 'Vermiculite', Clay Miner. 48 (4) (2013) 563-582, 10.1180/claymin.2013.048.4.01.

[75] D. Hillel, J.L. Hatfield, Encyclopedia of Soils in the Environment, Elsevier Amsterdam, 2005.

[76] D.L. Sparks, Environmental soil chemistry, Elsevier, 2003.

[77] I.E. Odom, Smectite clay minerals: properties and uses, Philos. Trans. Royal Soc. A PHILOS T R SOC A 311 (1517) (1984) 391-409, 10.1098/rsta.1984.0036.

[78] E. Castellini, D. Malferrari, F. Bernini, M.F. Brigatti, G.R. Castro, L. Medici, A. Mucci, M. Borsari, Baseline studies of the clay minerals society source clay montmorillonite STX-1b, Clays Clay Miner. 65 (4) (2017) 220-233, 10.1346/Ccmn.2017.064065.

[79] M. Lempart, A. Derkowski, K. Luberda-Durnas, M. Skiba, A. Blachowski, Dehydrogenation and dehydroxylation as drivers of the thermal decomposition of Fe-chlorites, Am. Mineral. 103 (11) (2018) 1837-1850, 10.2138/am-2018-6541.

[80] F. Villieras, J. Yvon, J.M. Cases, P. Dedonato, F. Lhote, R. Baeza, Development of Microporosity in Clinochlore Upon Heating, Clays Clay Miner. 42 (6) (1994) 679-688, 10.1346/Ccmn.1994.0420604.

[81] A. Steudel, R. Kleeberg, C.B. Koch, F. Friedrich, K. Emmerich, Thermal behavior of chlorites of the clinochlore-chamosite solid solution series: Oxidation of structural iron, hydrogen release and dehydroxylation, Appl. Clay Sci. 132 (2016) 626-634, 10.1016/j.clay.2016.08.013.

[82] J.E. Post, P.J. Heaney, Synchrotron powder X-ray diffraction study of the structure and dehydration behavior of palygorskite, Am. Mineral. 93 (4) (2008) 667-675, 10.2138/am.2008.2590.

[83] Y.-J. Huang, Z. Li, S.-Z. Li, Z.-L. Shi, L. Yin, Y.-F. Hsia, Mössbauer investigations of palygorskite from Xuyi, China, Nucl. Instrum. Methods Phys. Res. B: Beam Interact. Mater. At. 260 (2) (2007) 657-662, 10.1016/j.nimb.2007.04.218.

[84] K.L. Wang, L.J. Wang, Y. Zhang, Y.D. Zhang, J.S. Liang, Microstructural evolution and sintering properties of palygorskite nanofibers, Int. J. Appl. Ceram. Technol. 17 (4) (2020) 1833-1842, 10.1111/ijac.13485.

[85] T. Chen, J. Wang, C. Qing, S. Peng, Y. Song, Y. Guo, Effect of heat treatment on structure, morphology and surface properties of palygorskite, J. Chin. Ceram. Soc 34 (11) (2006) 1406-1410, 10.14062/j.issn.0454-5648.2006.11.022. (in Chinese).

[86] L. Boudriche, R. Calvet, B. Hamdi, H. Balard, Surface properties evolution of attapulgite by IGC analysis as a function of thermal treatment, Colloids. Surf. A Physicochem. Eng. 399 (2012) 1-10, 10.1016/j.colsurfa.2012.02.015.

[87] Y.D. Zhang, L.J. Wang, F. Wang, J.F. Sun, Q.G. Tang, J.S. Liang, Effects of palygorskite on physical properties and mechanical performances of bone china, Appl. Clay Sci. 168 (2019) 287-294, 10.1016/j.clay.2018.11.022.

[88] F.A. Andrade, H.A. Al-Qureshi, D. Hotza, Measuring the plasticity of clays: A review, Appl. Clay Sci. 51 (1-2) (2011) 1-7, 10.1016/j.clay.2010.10.028.

[89] J.M. Moreno-Maroto, J. Alonso-Azcárate, What is clay? A new definition of “clay” based on plasticity and its impact on the most widespread soil classification systems, Appl. Clay Sci. 161 (2018) 57-63, 10.1016/j.clay.2018.04.011.

[90] B. Tiwari, B. Ajmera, Consolidation and swelling behavior of major clay minerals and their mixtures, Appl. Clay Sci. 54 (3-4) (2011) 264-273, 10.1016/j.clay.2011.10.001.

[91] M. Dumbleton, G. West, Some factors affecting the relation between the clay minerals in soils and their plasticity, Clay Miner. 6 (3) (1966) 179-193, 10.1180/claymin.1966.006.3.05.

[92] A. Skempton, The colloidal activity of clays, Selected papers on soil mechanics (1953) 106-118.

[93] J.K. Mitchell, K. Soga, Fundamentals of soil behavior, John Wiley & Sons, New York, 2005.

[94] J. Bain, A plasticity chart as an aid to the identification and assessment of industrial clays, Clay Miner. 9 (1) (1971) 1-17, 10.1180/claymin.1971.009.1.01.

[95] Y. Zhang, L. Jia, H. Mei, Q. Cui, P. Zhang, Z. Sun, Fabrication, microstructure and properties of bricks fired from lake sediment, cinder and sewage sludge, Constr. Build. Mater. 121 (2016) 154-160, 10.1016/j.conbuildmat.2016.05.155.

[96] A. Polettini, R. Pomi, L. Trinci, A. Muntoni, S. Lo Mastro, Engineering and environmental properties of thermally treated mixtures containing MSWI fly ash and low-cost additives, Chemosphere 56 (10) (2004) 901-910, 10.1016/j.chemosphere.2004.05.004.

[97] H. Baccour, M. Medhioub, F. Jamoussi, T. Mhiri, Influence of firing temperature on the ceramic properties of Triassic clays from Tunisia, J. Mater. Process. Technol. 209 (6) (2009) 2812-2817, 10.1016/j.jmatprotec.2008.06.055.

[98] P. Chindaprasirt, A. Srisuwan, C. Saengthong, S. Lawanwadeekul, N. Phonphuak, Synergistic effect of fly ash and glass cullet additive on properties of fire clay bricks, J. Build. Eng. 44 (2021), 10.1016/j.jobe.2021.102942.

[99] E. Sallam, S. Naga, D. Ibrahim, Mode of talc addition and its effect on the properties of ceramic bodies, Ceram. Int. 10 (3) (1984) 87-92, 10.1016/0272-8842(84)90008-7.

[100] T.K. Mukhopadhyay, S. Ghosh, S. Ghatak, H.S. Maiti, Effect of pyrophyllite on vitrification and on physical properties of triaxial porcelain, Ceram. Int. 32 (8) (2006) 871-876, 10.1016/j.ceramint.2005.07.002.

[101] I.A.R. Barreto, M.L. da Costa, Sintering of red ceramics from yellow Amazonian latosols incorporated with illitic and gibbsitic clay, Appl. Clay Sci. 152 (2018) 124-130, 10.1016/j.clay.2017.11.003.

[102] J.F. Wu, K.Z. Tian, C.H. Wu, J.Q. Yu, H.L. Wang, J. Song, Q.N. Zhang, X.H. Xu, Effect of talc on microstructure and properties of the graphite tailing stoneware tiles, Constr. Build. Mater. 311 (2021) 125314, 10.1016/j.conbuildmat.2021.125314.

[103] S.A. Zaidan, S.S. Abdull-Razzak, Effect of bentonite addition on some properties of porcelain, J. Eng. 25 (1) (2019) 84-99.

[104] C.M.F. Vieira, S.N. Monteiro, Reformulation of a kaolinitic clay ceramic body with sand and flux clay for roofing tiles production, Mater. Sci. Forum, Trans Tech Publ, 2012, pp. 965-970.

[105] R. Chen, Y. Li, R. Xiang, S. Li, X. Fan, Y. Li, S. Sang, Effect of pyrophyllite addition on properties of lightweight insulation refractory materials, China's Refract. 26 (3) (2017) 38-42.

[106] T.K. Mukhopadhyay, S. Ghosh, M. Majumder, S. Ghatak, Consideration of Alternate Raw Materials for Porcelain Tile Manufacture: The Effect of the Incorporation of Fired Scrap and Pyrophyllite, InterCeram: Int. Ceram. Rev. 64 (1) (2015) 20-27.

[107] D. Njoya, M. Hajjaji, Effect of Addition of Talc on the Properties of Feldspar-Kaolinitic Clay Blends during Heating, Trans. Indian Ceram. Soc. 72 (4) (2013) 252-256, 10.1080/0371750x.2013.867645.

[108] T.K. Mukhopadhyay, M. Das, S. Ghosh, S. Chakrabarti, S. Ghatak, Microstructure and thermo mechanical properties of a talc doped stoneware composition containing illitic clay, Ceram. Int. 29 (5) (2003) 587-597, 10.1016/S0272-8842(02)00206-7.

[109] B. Beal, A. Selby, C. Atwater, C. James, C. Viens, C. Almquist, A Comparison of Thermal and Mechanical Properties of Clay Bricks Prepared with Three Different Pore-Forming Additives: Vermiculite, Wood Ash, and Sawdust, Environ. Prog. Sustain. 38 (6) (2019) 13150, 10.1002/ep.13150.

[110] C. Bories, M.E. Borredon, E. Vedrenne, G. Vilarem, Development of eco-friendly porous fired clay bricks using pore-forming agents: A review, J. Environ. Manag. 143 (2014) 186-196, 10.1016/j.jenvman.2014.05.006.

[111] G. Cultrone, E. Sebastian, K. Elert, M.J. de la Torre, O. Cazalla, C. Rodriguez-Navarro, Influence of mineralogy and firing temperature on the porosity of bricks, J. Eur. Ceram. Soc. 24 (3) (2004) 547-564, 10.1016/S0955-2219(03)00249-8.

[112] W. Qingbo, L. Liqiang, Z. Dong, Z. Quanpeng, W. Mingguo, N. Wenhe, Influence of bentonite dosage on the properties of fly ash-red mud porous ceramics, China Ceramics 49 (3) (2013) 56-58.

[113] S. Ergul, M. Akyildiz, A. Karamanov, Ceramic material from basaltic tuffs, Ind. Ceram. 27 (2) (2007) 89-94.

[114] H. Boussak, H. Chemani, A. Serier, Characterization of porcelain tableware formulation containing bentonite clay, Int. J. Phys. Sci. 10 (1) (2015) 38-45.

[115] M. Sutcu, Influence of expanded vermiculite on physical properties and thermal conductivity of clay bricks, Ceram. Int. 41 (2) (2015) 2819-2827, 10.1016/j.ceramint.2014.10.102.

[116] J.F. Clifford, High temperature reactions and colour development in brick clays, University of Surrey (United Kingdom), 1984.

[117] J.D. Bautista-Marin, A. Esguerra-Arce, J. Esguerra-Arce, Use of an industrial solid waste as a pigment in clay bricks and its effects on the mechanical properties, Constr. Build. Mater. 306 (2021) 124848, 10.1016/j.conbuildmat.2021.124848.

[118] R. Kreimeyer, Some notes on the firing colour of clay bricks, Appl. Clay Sci. 2 (2) (1987) 175-183, 10.1016/0169-1317(87)90007-X.

[119] G. Cultrone, The use of Mount Etna volcanic ash in the production of bricks with good physical-mechanical performance: Converting a problematic waste product into a resource for the construction industry, Ceram. Int. 48 (4) (2022) 5724-5736, 10.1016/j.ceramint.2021.11.119.

[120] M.V. Vasic, L.L. Pezo, J.D. Zdravkovic, M. Vrebalov, Z. Radojevic, Thermal, Ceramic and Technological Properties of Clays used in Production of Roofing Tiles - Principal Component Analysis, Sci. Sinter. 50 (4) (2018) 487-500, 10.2298/Sos1804487v.

[121] P. Munoz, V. Letelier, M.A. Bustamante, J. Marcos-Ortega, J.G. Sepulveda, Assessment of mechanical, thermal, mineral and physical properties of fired clay brick made by mixing kaolinitic red clay and paper pulp residues, Appl. Clay Sci. 198 (2020) 105847, 10.1016/j.clay.2020.105847.

[122] L. Crespo-López, G. Cultrone, Improvement in the petrophysical properties of solid bricks by adding household glass waste, J. Build. Eng. 59 (2022) 105039, 10.1016/j.jobe.2022.105039.

[123] J. Garcia-Ten, M.J. Orts, A. Saburit, G. Silva, Thermal conductivity of traditional ceramics Part II: Influence of mineralogical composition, Ceram. Int. 36 (7) (2010) 2017-2024, 10.1016/j.ceramint.2010.05.013.

[124] M. Arsenovic, Z. Radojevic, S. Stankovic, Z. Lalic, L. Pezo, What to expect from heavy clay?, Ceram. Int. 39 (2) (2013) 1667-1675, 10.1016/j.ceramint.2012.08.009.

[125] M.L. Gualtieri, A.F. Gualtieri, S. Gagliardi, P. Ruffini, R. Ferrari, M. Hanuskova, Thermal conductivity of fired clays: Effects of mineralogical and physical properties of the raw materials, Appl. Clay Sci. 49 (3) (2010) 269-275, 10.1016/j.clay.2010.06.002.

[126] J.G. Ten, M.J. Orts, A. Saburit, G. Silva, Thermal conductivity of traditional ceramics. Part I: Influence of bulk density and firing temperature, Ceram. Int. 36 (6) (2010) 1951-1959, 10.1016/j.ceramint.2010.05.012.

[127] E. Galan, Genesis of Clay Minerals, In: F. Bergaya, G. Lagaly (Eds.), Handbook of Clay ScienceNewnes, 2006, pp. 1129-1162.

[128] I. Tole, K. Habermehl-Cwirzen, A. Cwirzen, Mechanochemical activation of natural clay minerals: an alternative to produce sustainable cementitious binders - review, Mineral. Petrol. 113 (4) (2019) 449-462, 10.1007/s00710-019-00666-y.

Highlights

- The crucial role of clay minerals in brick production is highlighted.
- Thermal behaviors of 8 clay minerals relevant to brick manufacture are summarized.
- The effects of clay minerals on fired brick properties are comprehensively reviewed.
- Multi-disciplinary perspectives are adopted covering building materials, ceramics, and mineralogy.
- Current challenges and outlooks on clay mineral-based brick products are proposed.

CRediT authorship contribution statement

Sen Wang: Conceptualization, Methodology, Writing - original draft. **Lloyd Gainey:** Methodology, Resources, Formal analysis. **Ian D.R. Mackinnon:** Project administration, Supervision, Writing - review & editing. **Charlotte Allen:** Methodology, Writing - review & editing. **Yuantong Gu:** Writing - review & editing. **Yunfei Xi:** Conceptualization, Methodology, Project administration, Supervision, Funding acquisition, Writing - review & editing.

Declaration of interests

☒ The authors declare that they have no known competing financial interests or personal relationships that could have appeared to influence the work reported in this paper.

☐The authors declare the following financial interests/personal relationships which may be considered as potential competing interests: